The long-term performance of a bituminous geomembrane (BGM) under single-sided exposure conditions

F. B. Abdelaal*[1], A. Samea[2]

*Corresponding author

[1]Assistant Professor in Geotechnical and Geoenvironmental Engineering, GeoEngineering Centre at Queen's-RMC, Queen's University, Ellis Hall, Kingston ON, Canada K7L 3N6. E-mail: fady.abdelaal@queensu.ca, Phone: (613) 533-3352. Fax: (613) 533-2128.

[2]PhD Student, GeoEngineering Centre at Queen's-RMC, Queen's University, Kingston ON, Canada, K7L 3N6. E-mail: alireza.samea@queensu.ca

ABSTRACT

A custom-designed apparatus (referred to as the Ageing Column) is used to age a 4.8-mm thick elastomeric bituminous geomembrane (BGM) under single-sided exposure to a synthetic municipal solid waste (MSW) leachate and a synthetic high pH mining solution (pH 11.5) at 55, 70, and 85°C. This apparatus involves a closer simulation of the BGM's chemical exposure conditions in the field than the double-sided immersion tests in which the BGM is exposed to the solution from both surfaces. The mechanical, rheological, and chemical properties of the BGM are examined to assess the degradation in the BGM components relative to double-sided immersion experiments. While the single-sided ageing of the BGM reduces the degradation rates in the BGM mechanical properties, it does not affect the degradation rate of the bitumen coat relative to the double-sided exposure. Additionally, the exposure of the BGM to the MSW leachate resulted in faster degradation in its mechanical properties but slower degradation in the bitumen coat than that obtained in the exposure to the mining solution. However, predictions of the time to nominal failure of the BGM established using Arrhenius modelling at different temperatures show that the temperature effect is more significant on the BGM durability than the chemistry of the considered solutions.

Keywords: Geosynthetics, Bituminous Geomembrane, Landfill Liners, Heap Leach Pads, Service Life.

1. Introduction

Waste containment applications such as municipal solid waste (MSW) landfills and mineral resource extraction applications such as heap leach pads are required to be constructed on geosynthetic barrier systems. These systems typically consist of a geomembrane (GMB) liner overlying a low hydraulic conductivity layer (either a geosynthetic clay liner (GCL) or compacted clay liner (CCL)) (Rowe et al. 2004; Rowe 2005; Lupo 2010; Tian et al. 2014). Composite barrier systems are designed and constructed to minimize the contaminant transport into the surrounding environment during the design life of these different facilities. A key factor that controls the efficacy of the liner system in these different geoenvironmental applications is the chemical durability of the GMB liner. With the various GMB materials available in the market, it is necessary to assess their chemical compatibility with the solutions in the field to ensure adequate environmental protection.

Bituminous geomembranes (BGMs) are among the different GMB products that are used in hydraulic and containment applications. BGMs comprise a polyester nonwoven geotextile (NW-GTX) and a glass fleece mat impregnated and coated with bitumen to give a relatively impervious sheet with high mechanical properties. The bitumen used in manufacturing BGMs is typically modified with polymer additives (e.g., styrene-butadiene-styrene (SBS) copolymer) to increase its workable range of temperature and improve its temperature sensitivity (Scheirs 2009; Zhu et al. 2014; Touze-Foltz and Farcas 2017). To improve the interface friction resistance of the BGM with the soil/geosynthetic material above it, the top surface of the BGM is often treated with fine sand. A polyester (PET) film is bonded to the bottom side of the BGM, to prevent the material from adhering to itself during storage in rolls and to protect it from upward root penetration while in service (Lazaro and Breul 2014).

The applications of BGMs have evolved from being limited to hydraulic applications such as canal liners to their growing use over the last two decades as the primary liner and cover material for different geoenvironmental applications. For example, BGMs have been used in lining and capping municipal solid waste (MSW) and low-level radioactive waste (LLRW) landfills (Breul et al. 2006; Peggs 2008; Daly and Breul 2017; Keys 2021; Richardson and Wingrove 2021). They have also been introduced to mining applications to line mine process solution spillover lagoons, mine tailings storage facilities, and heap leach pads (Scheirs 2009; Lazaro and Breul 2014; Daly and Breul 2017). The growing use of BGMs is attributed to their favourable material characteristics, such as high resistance to punctures, flexibility at lower temperatures, low coefficient of thermal expansion, and higher density relative to polymeric GMBs (Breul et al. 2008; Peggs 2008; Lazaro and Breul 2014). However, there is a paucity of research examining their chemical durability under the different exposure conditions of these geoenvironmental applications.

Very few studies have been conducted on field-exhumed samples to assess the long-term performance of BGMs in geoenvironmental applications (e.g., Addis et al. 2013; Touze-Foltz and Farcas 2017). For instance, Touze-Foltz and Farcas (2017) examined the durability of a BGM after 30 years in water ponds exposed to an average annual temperature ranging from 6.1 to 15.3^{o}C. Despite exhibiting degradation in the bitumen coat within the first few microns from the surface, the tensile properties of the exhumed samples were not affected after 30 years of exposure, and they maintained the same waterproofing characteristics of a virgin BGM. Few recent laboratory studies have been also conducted on BGMs using immersion tests in which the BGM coupons are immersed in stainless steel containers filled with the desired solution at different elevated temperatures to explore their degradation behaviour and predict their longevity

at field temperatures in different geoenvironmental applications (e.g., Samea and Abdelaal 2023a; Abdelaal and Samea 2023; Samea and Abdelaal 2023b). These studies showed that at elevated temperatures, BGMs exhibit degradation in their mechanical, chemical, and rheological properties upon incubation since they are not typically formulated with antioxidants. Such degradation of the multicomponent BGMs progresses simultaneously in the bitumen coat and the NW-GTX and the extent of the degradation in these different components depends on the incubation media. These studies allowed the estimation of the time nominal failure of BGMs based on the loss of the mechanical and viscoelastic properties when exposed to different incubation media. While the double-sided exposure of the BGM in these studies simulates the exposure conditions for a punctured liner that can become exposed to the solution from both surfaces, the estimates of the time to nominal failure are expected to be shorter than those in the field for an intact liner. This is because an intact BGM is exposed to the solution in the field from the bitumen coat side only (referred to as single-sided exposure herein).

To assess the longevity of an intact GMB in the laboratory, previous studies examined the durability of polymeric GMBs under simulated field conditions as part of a composite liner system (e.g., Hsuan and Koerner 1998; Brachman et al. 2008; Rowe and Rimal 2008; Rowe et al. 2010; Rowe et al. 2013; Abdelaal et al. 2014a). These studies allowed the comparison of the degradation rates obtained from the double-sided immersion to the single-sided field exposure conditions. For instance, Rowe and Rimal (2008) examined the antioxidant depletion from a 1.5 mm high density polyethylene (HDPE) GMB underlying a NW-GTX protection layer and overlaying a GCL using 160 mm diameter stainless steel cells. The results from this composite liner setup that did not involve applied stresses were compared to those obtained from immersion tests using the same GMB and leachate. It was shown that the rate of antioxidant depletion in the leachate-immersed

GMBs at different temperatures was approximately 2.2-4.8 times faster than that of GMBs in the simulated composite liner system.

A closer simulation of the field conditions was presented by Rowe et al. (2010; 2013) using 600 mm diameter stainless steel cells by examining a 1.5 mm HDPE GMB in a composite liner configuration under an overburden pressure of 250 kPa and with leachate circulation in the drainage layer. With a 580 g/m^2 NW-GTX protection, the average ratio of the antioxidant depletion rate for the same GMB immersed in leachate to that in the composite liner at different temperatures was approximately 4.8. Additionally, when a 200 g/m^2 NW-GTX and 150 mm thick sand protection layer was used, the average immersion to composite liner depletion ratio was increased to 7.7.

Due to the complexity of these large scale tests, limited availability, and long testing times, immersion tests are still widely used to explore testing variables such as different solution chemistries and different GMB formulations (e.g., Gulec et al. 2004; Jeon et al. 2008; Abdelaal et al. 2014b; Ewais et al. 2014; Tian et al. 2017; Vahidi et al. 2020; Morsy et al. 2021; Li et al. 2021; Li et al. 2021; Abdelaal and Rowe 2023; Rowe and Somuah 2023; Zafari et al. 2023). The degradation rates obtained from these double-sided immersion studies can be then shifted to single-sided degradation in the field using the aforementioned factors obtained from the large scale tests (e.g., Rowe et al. 2020; Abdelaal and Rowe 2023). However, these shift factors cannot be generalized to all testing conditions especially when the durability of GMBs with different types or compositions is examined.

Unlike the traditional monolayer polymeric GMBs, BGMs are composite materials with an asymmetric structure as described earlier. As such, the BGMs may exhibit different resistance to degradation depending on the surface exposed to the solution. Thus, the shift factors (from

degradation in double-sided and single-sided exposures) obtained from the previous polymeric GMB research cannot be used to accurately predict the BGM performance in field exposure conditions. Therefore, the first objective of the current study is to investigate the effect of the field single-sided exposure conditions relative to the double-sided exposure on the degradation behaviour of a BGM at different temperatures and for different exposure media. The second objective is to provide improved estimates of the time to nominal failure obtained from previous studies that aged BGMs in double-sided immersion by considering the field single-sided exposure conditions.

2. Experimental investigation

2.1 Accelerated ageing method

To simulate the field exposure conditions in the laboratory, a custom-designed apparatus (denoted as the Ageing Column; Figure 1) was assembled to age BGMs in a single-sided exposure, at different elevated temperatures. The apparatus consists of 300x300 mm square stainless steel sections that are 100 mm in height, and with 400 mm flanges. A 400 mm square BGM sample was placed between every two sections and supported over two 2.0-mm thick HDPE GMBs to ensure the BGM remains flat and prevents any exposure to the solution from the bottom surface. Stainless steel bolts were used to secure the BGM between the flanges of the two sections. The sections were assembled on top of each other to build an Ageing Column with 5 BGM specimens. The desired immersion solution was introduced through ports located in each section above the BGM to allow exposure of the BGM to solutions from the top bitumen coat side only. The solution head was approximately 20 mm above the BGM which was the same for each BGM sample in the different sections of the Ageing Column. The low solution head was chosen to ensure that it does not result in the bending of the BGM sample while the solution remains in contact with the

entire BGM surface during the entire duration of the solution refreshment cycles. Although this apparatus does not simulate the composite liner exposure conditions that involve a GCL/CCL under the BGM, it represents a closer simulation of field conditions than double-sided immersion tests.

Experiments were conducted at three elevated temperatures (55, 70, and 85^{o}C) to accelerate the ageing of the BGM and to allow comparing the results to those obtained from previous immersion studies for the same BGM (i.e., Abdelaal and Samea 2023; Samea and Abdelaal 2023b). In the asphalt industry, accelerated ageing tests, such as the rolling thin film and the pressure ageing vessel, typically involve temperatures ≥ 100°C to evaluate the thermo-oxidation degradation of stabilized bitumen (e.g., Lu et al. 2008; Mouillet et al. 2011; Aguiar-Moya et al. 2017; Kaya et al. 2020). However, to minimize any significant material changes in the various components of the BGM during ageing (especially the bitumen), the highest temperature in this study was limited to 85°C since it is around 20^{o}C below the typical melting point reported for SBS-modified bitumen (Cheng et al. 2019; Cong et al. 2021). This also simulates the reported temperature in the field by Addis et al. (2013) for a BGM liner installed in South America.

A self-regulating heating cable was wrapped around each column and connected to a temperature controller to heat the column at the desired temperature. Insulation jackets were then used to cover the entire surface of the column to minimize heat loss. The temperatures of each section were monitored using a thermocouple attached to each section at the BGM to ensure the actual BGM temperature was maintained at ±1^{o}C of the set temperature. BGM specimens were extracted from the Ageing Column at different incubation durations to monitor their degradation using different index tests.

2.2 BGM examined

The BGM examined (TERANAP 531-4M; Table 1) has a nominal thickness of 4.8 mm with a mass per unit area of 5410 g/m^2. The reinforcement layers involve a polyester NW-GTX with a mass per unit area of 275 g/m^2 and a glass fleece mat with a mass per unit area of 50 g/m^2 both impregnated and coated with SBS-modified bitumen. According to the BGM manufacturer, the glass fleece mat is added to improve the dimensional stability of the BGM roll during manufacturing and service with limited contribution to its mechanical properties. The top bitumen surface of the BGM was coated with sand, while the bottom surface was bonded to a PET film. Due to its high initial mechanical properties, the BGM examined is recommended by the manufacturer for various geoenvironmental applications, including lining and capping MSW landfills and heap leach pads (Daly et al. 2018; Keys 2021; Richardson and Wingrove 2021).

2.3 Immersion solutions

Two different synthetic solutions (Table 2) were examined that simulate MSW landfill leachate and a high pH mining solution. These two solutions were selected since they were used in previous immersion studies conducted on the same BGM (Abdelaal and Samea 2023; Samea and Abdelaal 2023b) to allow comparing the performance in double-sided and single-sided (Ageing Column) immersion tests. The synthetic MSW leachate is reduced (Eh =-120 mV) to simulate anaerobic leachates found in MSW landfills and composed of inorganic/organic salts, a trace metals solution, and an industrial surfactant based on a chemical analysis of leachate from a landfill in Ontario, Canada (Hrapovic 2001). The synthetic mining solution examined simulates the pregnant leach solutions in gold and silver heap leaching operations with a pH of 11.5 (denoted as PLS pH 11.5). The PLS pH 11.5 was prepared by mixing inorganic salts with deionized water and titrating sodium hydroxide (15M) to achieve the desired pH. The two

solutions were replaced every two months to ensure a constant pH and chemistry of the solutions throughout the study.

3. Index testing methods

3.1 Rheology and chemical index tests

Different chemical and rheological index tests were used to examine the changes in the different properties of the bitumen due to chemical degradation using the unaged and aged samples at different incubation times and temperatures. These tests have been widely used in asphalt research to explore the degradation of stabilized bitumen when exposed to service conditions (Airey 2003; Aguiar-Moya et al. 2017; Kaya et al. 2020; Mark et al. 2004; Puello et al. 2013; Yu et al. 2019). In the current study, these tests were used to characterize the degradation in the bitumen coat of the BGM aged under conditions that are relevant to geoenvironmental applications.

3.1.1 Modulated differential scanning calorimetry

A modulated differential scanning calorimeter equipped with a refrigerated cooling system was used to evaluate the changes in the glass transition temperature (T_g) of the aged bitumen coat of the BGM according to the inflection method (ASTM E2602). A sample of 5-8 mg was encapsulated in Tzero hermetic pans with hermetic lids. In the first heating cycle, the sealed pans were heated from 20°C to 170°C at a rate of 5°C/min and conditioned for 15 minutes under a constant flow (50 mL/min) of nitrogen. This was followed by a cooling rate of 10°C/min to reach -110°C. This procedure allowed removing any previous thermal history during the manufacturing of the bitumen (Frolov et al. 2019). In the second heating cycle, the samples were heated to 170°C at a rate of 5°C/min while modulating the temperature with the accuracy of ± 0.75°C every 60 seconds. Three replicates were tested for each aged data point at different incubation times.

3.1.2 Dynamic shear rheometer

To monitor the effect of ageing on the rheological properties of bitumen, dynamic mechanical analysis was carried out using a Dynamic Shear Rheometer (DSR). This test is widely used to determine the complex shear modulus (G^*) and phase angle (δ) of bituminous materials to provide information about the changes in their viscous and elastic behaviours due to ageing. G^* represents the ratio of the absolute shear stress and the resulting shear strain and is known as a measurement of the stiffness of the material, while δ is a relative measurement of the viscous and elastic properties of a material that represents the degree of fluidity (Airey 2003). The specimens were subjected to a constant normal force of 1 N and a steady oscillation frequency of 10 rad/s while being held between two 25 mm parallel circular plates at 55°C. Both G^* and δ were recorded in the linear viscoelastic region (LVE), since the bitumen exhibits stability in the values of G^* and δ at relatively low strains. Three replicates were tested for samples collected at each incubation duration.

3.1.3 Fourier transform infrared spectroscopy

Fourier Transform Infrared (FTIR) analysis was conducted to identify the changes in the functional groups of the bitumen coat due to ageing. The FTIR analysis was conducted with a resolution of 4 cm^{-1}, at wavenumber ranging between 4000-400 cm^{-1} and a total of 32 scans per sample were performed (e.g., Lamontagne et al. 2001; Frolov et al. 2019; Wang et al. 2019; Zhang et al. 2021). To verify the reproducibility of the results, quadruplicate specimens were examined for each data point at 22°C. The FTIR samples were prepared by extracting a sample from the bitumen coat and fully dissolving it in toluene (10% bitumen by mass). The bitumen solution was then applied and dried on a potassium bromide disk and examined in the FTIR.

Previous studies (e.g., Durrieu et al. 2007; Zeng et al. 2015; Yu et al. 2019) showed that thermal degradation of the bitumen can be inferred from the increase in the carbonyl (C=O) functional groups (centred around 1700 cm^{-1}), while the SBS copolymer degradation can be inferred from the change in the butadiene double bonds (C=C; centred around 968 cm^{-1}). Thus, the degree of ageing of the bitumen coat of the BGM was characterized using the carbonyl and butadiene indices (e.g., Lamontagne et al. 2001; Gao et al. 2013; Feng et al. 2022; Su et al. 2023) that can be calculated viz:

$$I_{C=O} = \frac{Area\ of\ the\ carbonyl\ band\ centered\ around\ 1700\ cm^{-1}}{\Sigma Area\ of\ the\ spetral\ bands\ between\ 4000\ and\ 600\ \ cm^{-1}} \quad \text{(Eq 1)}$$

$$I_{SBS} = \frac{Area\ of\ the\ carbonyl\ band\ centered\ around\ 968\ cm^{-1}}{\Sigma Area\ of\ the\ spetral\ bands\ between\ 4000\ and\ 600\ \ cm^{-1}} \quad \text{(Eq 2)}$$

Where; $I_{C=O}$ = carbonyl index and I_{SBS} = butadiene index.

3.2 Mechanical index tests

Tensile and puncture properties of the unaged and aged BGM were measured at room temperature (22°C) to evaluate the degradation in the NW-GTX reinforcement layer of the BGM. Tensile tests were conducted using a universal testing machine with initial machine grips separation of 60 mm and at a constant strain rate of 50 mm/min (ASTM D7275). The maximum stress and the corresponding elongation were recorded as the tensile strength and elongation per the ASTM D7275 test method since these values reflect the onset of failure of the NW-GTX. The puncture resistance was evaluated using a loading machine in compliance with ASTM D4833 at a strain rate of 50 mm/min. The maximum force and corresponding elongation were recorded as the index static puncture properties of the BGM.

4. Results and discussion

4.1 Effect of single-sided exposure at 70°C on the chemical and rheological properties of the bitumen coat

The changes in the T_g of the bitumen coat resulting from the exposure to the PLS pH 11.5 and the MSW leachate in single-sided exposure are compared to the double-sided immersion in Figure 2. In the two ageing experiments, the T_g of the bitumen decreased linearly as the incubation time increased in both solutions. This behaviour is likely caused by the thermo-oxidative degradation altering the structure of the bitumen at 70°C (e.g., Lu and Isacsson 2002; Yu et al. 2014; Bachir et al. 2016; Kaya et al. 2020). The values obtained from the single-sided exposure to PLS pH 11.5 and MSW leachate showed that the T_g of the unaged bitumen (-24.2°C) decreased over the 18 months of exposure to reach -35°C and -32°C, respectively. Notably, a similar T_g was achieved in the double-sided exposure after the same ageing duration in both media (Figure 2). Comparing the results in both solutions under different exposure conditions suggests that the ageing method (either single or double-sided) did not affect the oxidative degradation of the bitumen coat.

For the rheological properties of the bitumen, upon incubation at 70°C, exposure to both the PLS pH 11.5 and the MSW leachate resulted in a gradual increase in G^* to reach 2.1 and 1.6 times the initial G^* after 18 months, respectively (Figure 3a and 3c). Concurrently, the values of δ decreased by 30% in PLS pH 11.5 and by 19% in the MSW leachate (Figure 3b and 3d). The changes in G^* and δ with ageing imply the increase in the bitumen rigidity as it shifts toward a more elastic behaviour. Additionally, the rate of changes in these values in the single-sided experiments was similar to those reported by Abdelaal and Samea (2023) and Samea and Abdelaal (2023b) for double-sided immersion. This suggests that the ageing method did not significantly affect the changes in the viscoelastic properties of the bitumen coat.

For the results obtained from the FTIR analysis, the $I_{C=O}$ of unaged bitumen (0.0024) increased with the single-sided exposure to the PLS pH 11.5 and MSW leachate at 70°C after 18 months of incubation by factors of 6 and 4.1, respectively (Figure 4a and 4c as a result of the thermo-oxidative degradation of the bitumen coat (Yang et al. 2018). In contrast, I_{SBS} decreased in both solutions, reaching 75% and 85% of the initial value in the PLS pH 11.5 and MSW leachate, respectively, implying a degradation in the SBS-copolymer stabilizing the bitumen coat (Figure 4b and 4d).

The FTIR results were consistent with the T_g, G^* and δ showing that the rate of the bitumen degradation in the single-sided exposure experiments was similar to the double-sided immersion reported by Abdelaal and Samea (2023) and Samea and Abdelaal (2023b). Thus, the ageing method did not affect the rate of oxidative degradation of the bitumen coat. Furthermore, the rate of degradation in all the chemical and rheological properties of the bitumen was faster when exposed to the PLS pH 11.5 than the MSW leachate.

4.2 Effect of single-sided exposure at 70°C on the degradation in the mechanical properties of the BGM

For the single-sided aged BGM samples in PLS pH 11.5 at 70°C, the maximum (peak) tensile strength (σ_{max}) remained unchanged for the first 5 months of the incubation period. This was followed by a gradual decrease over time to reach 55% of the initial value after 18 months (Figure 5a). In the MSW leachate, and without any initial retention period, σ_{max} decreased linearly over the 18-month incubation period reaching 10% of the initial value (Figure 5c). For the tensile elongations at maximum strength (ε_{max}), there was a gradual decrease in the values after exposure to both solutions without any retention period (Figures 5b and 5d). In PLS pH 11.5 , ε_{max} decreased to reach 45% of the initial value after 18 months while the degradation rate was faster in MSW

leachate in which ε_{max} decreased to 8% of the initial value after the same incubation duration. Similar to the tensile test results, the puncture resistance of the single-sided aged BGM in the PLS pH 11.5 and MSW leachate decreased to 65% and 15% of the initial values, respectively, after 18 months (Figures 6a and 6c). Likewise, the puncture elongation at the maximum force was reduced to 70% and 50% of the initial values after 18 and 12 months in the PLS pH 11.5 and MSW leachate, respectively (Figures 6b and 6d).

Figures 5 and 6 show that the degradation in tensile and puncture properties of the BGM obtained from the double-sided immersion tests was faster than that obtained from the single-sided immersion. For example, σ_{max} and ε_{max} of the double-sided immersed samples in PLS pH 11.5 after 18 months of incubation at 70°C degraded to approximately 18% and 8% of their initial values, respectively. For the single-sided immersed samples and after the same exposure duration at 70°C, the BGM exhibited less degradation reaching 55% and 45% of its initial σ_{max} and ε_{max}, respectively. Likewise, for the MSW leachate, σ_{max} reached 10% of the initial value after 11 months for the double-sided immersed samples while the same value was reached after 15 months for the single-sided immersed samples. Although the degradation in the MSW leachate was still slower in the single-sided than the double-sided exposure, the differences in the degradation rates between the two exposure conditions were smaller than those observed in the PLS pH 11.5 . Thus, the rate of degradation in the NW-GTX was affected by the ageing method and the chemistry of the exposure solution.

4.3 Discussion of the BGM degradation behaviour in single-sided exposure condition

Exposure of the BGM to the PLS pH 11.5 and the MSW leachate from the top surface of the BGM at elevated temperatures resulted in changes in the chemical and rheological properties of the bitumen coat. These changes are attributed to the thermo-oxidative degradation of the

bitumen, which increased the carbonyl functional groups ($I_{C=O}$), and the scissioning of the chains of the SBS copolymer implied from the reduction in the butadiene functional groups (I_{SBS}). The thermo-oxidative degradation of the bitumen also increased its stiffness (increase in G^* with the reduction in δ) and ultimately led to the cross-linking of bitumen molecules implied from the changes in its T_g (Liu et al. 2003; Omairey et al. 2020). Although the changes in the chemical and rheological properties of the bitumen coat increased with the increase in the incubation time, the BGM started to exhibit degradation in its mechanical properties at early incubation times at 70°C (Figure 7). This implies that in aqueous solutions at 70°C, the chemical constituents of the solution can interact with the bitumen-coated and fully impregnated NW-GTX even with the slight degradation in the bitumen coat observed at the early incubation times. Thus, the degradation of the BGM in the solutions examined herein involved concurrent degradation in its different components that took place once the BGM was incubated at elevated temperatures.

The degradation behaviour of BGMs discussed above for the single-sided exposure is similar to that observed in the double-sided experiments. However, the relative degradation between these two exposure conditions was different for the different components of the BGM. For the bitumen coat, the double-sided and single-sided immersed BGM samples exhibited the same degradation in all the chemical and rheological properties. This implies that the extent of degradation in the chemical and rheological properties of the BGM in the double-sided exposure is only affected by the solution in contact with the bitumen coat. Among all the constituents of the aqueous solutions that can accelerate the degradation of the bitumen coat (i.e., pH, chemical constituents, and dissolved oxygen), it seems that dissolved oxygen had the greatest effect. This is because, for the same BGM immersed in air, Samea and Abdelaal (2023a) reported a 12.5-fold increase in $I_{C=O}$ after 18 months, while the double-sided immersed BGM exhibited a 6- and 4.1-

fold increase in $I_{C=O}$ in PLS pH 11.5 (non-reduced with Eh=+115 mV) and MSW leachate (reduced with Eh=-120 mV), respectively. This also implies that exposing the bottom PET film to the solution in double-sided immersion may have inhibited the direct exposure of the bitumen to the dissolved oxygen from the bottom surface of the BGM. Although the PET was still attached to BGM during the entire duration of this study, it is expected that the rate of degradation of the entire bituminous component of the BGM may become faster in the double-sided than in the single-sided immersion if the PET film is completely degraded or detached from the BGM. Thus, the estimates of the degradation times of the bitumen coat obtained from double-sided immersion tests can be used to estimate the bitumen coat degradation under single-sided field conditions as long as the PET film protects the bottom surface of the BGM.

For the degradation in the mechanical properties, exposure of the BGM to the solution from the top surface resulted in a slower degradation than those obtained from the double-sided immersion in PLS pH 11.5 and MSW leachate. The degradation in the mechanical properties of BGMs in aqueous solutions can be attributed to the degradation of the polyester fibres of the NW-GTX by hydrolysis (Samea and Abdelaal 2023a). This degradation can only occur when the H^+/ OH^- ions from the solution diffuse into the BGM to interact with the NW-GTX even with a slightly degraded bitumen coat. Since the double-sided coupons were sealed at the edges with BGM strips that were welded to coupons to ensure that the coupons were only in direct contact with the solution from the top and bottom sides (Samea and Abdelaal 2023a; Abdelaal and Samea 2023), it seems that PET film did not essentially protect the NW-GTX from degradation by hydrolysis. However, another plausible explanation is that the PET inhibited the degradation of the NW-GTX from the bottom surface while the solution constituents resulting in hydrolysis of NW-GTX fibres still diffused through the sealing strips and degraded the NW-GTX from the

edges. Either or both explanations could be valid since the degradation in the mechanical properties of the double-sided immersed BGM samples was similar to the degradation of the NW-GTX that was used in the formulation of the BGM and separately incubated in the PLS pH 11.5 and MSW leachate (Figure 8). These degradation rates were faster than that of the single-sided immersed BGM samples in which the constituents of the solutions can only diffuse from the top bitumen coat. Thus, estimates of the degradation times in the mechanical properties from the double-sided immersion of BGM are more conservative (i.e., shorter) than those expected in the field with single-sided exposure to the solution.

Considering the effect of the different solutions, in the PLS pH 11.5 , the difference in the degradation rate in mechanical properties (e.g., Figures 6a and 6b) between the single-sided and double-sided immersion was much greater than in MSW leachate (e.g., Figures 6c and 6d). The small difference in the degradation rates in the two immersion tests in the MSW leachate can be attributed to the presence of surfactant that increases the surface wettability of BGM (Rowe et al. 2009). This can potentially increase the interaction between the chemical constituents of the MSW leachate and the NW-GTX from the BGM top surface than the chemical constituents of the PLS pH 11.5 without surfactant. This highlights that the difference in the degradation of the mechanical properties between the double-sided immersion tests and single-sided field exposure is dependent on the chemistry of the solution in contact with the BGM surface.

In summary, the previous results show that the BGM's reinforcement layer is the only component that was sensitive to the immersion method thereby showing faster degradation in the double-sided than the single-side immersion. Additionally, the faster degradation rates of rheological and chemical properties in the PLS pH 11.5 than in the MSW leachate can be attributed to the reduced conditions of the MSW leachate while the faster degradation rates of

mechanical properties in MSW leachate than in PLS pH 11.5 can be attributed to the presence of surfactant in the MSW leachate.

5. Temperature effect on the BGM degradation and estimation of the time to nominal failure

In addition to the 70°C experiments presented in the previous sections, the Ageing Column experiments were conducted at 55 and 85°C to evaluate the effect of incubation temperature on the different properties of the BGM. The results obtained from exposure to both the PLS pH 11.5 and MSW leachate showed that an increase in the exposure temperature resulted in faster changes in the chemical, rheological, and mechanical properties of BGM. For instance, Figure 9 shows that the BGM exhibited degradation in G^* at all incubation temperatures including the 55°C with the rates of degradation (i.e., the slope of the best fit lines) increasing with the increase in temperature. Additionally, these degradation rates in PLS pH 11.5 were faster than in the MSW leachate due to reduced conditions of the MSW leachate discussed in Section 4.3.

For the mechanical properties, degradation in ε_{max} in both the PLS pH 11.5 and MSW leachate was only observed at 70 and 85°C while ε_{max} was retained at the initial value in both solutions at 55°C during the 18-month monitoring period (Figure 10). Due to the previously discussed effect of surfactant in the MSW leachate, the degradation rates of ε_{max} obtained at 70 and 85°C in the MSW leachate were faster than those obtained in the PLS pH 11.5 . However, irrespective of the solution, the degradation in mechanical properties at elevated temperatures (i.e., 70 and 85°C) occurred at fast rates and the mechanical resistance of the BGM reached very low values after short incubation times. These results highlight the significant effect of elevated temperatures on the degradation of the mechanical properties of the BGM.

Although the single-sided experiments simulated the field chemical exposure conditions (i.e., exposure to the chemical solution from the top surface only), the stresses on the BGM were not simulated in these experiments. In this case, the degradation rates obtained from these experiments cannot reflect the service life (i.e., time to rupture) of the BGM in the field that is related to the loss of its hydraulic barrier function. Instead, these degradation rates can be used to estimate the time to nominal failure (t_{NF}) of the BGM material when it reaches low resistance due to degradation. For polymeric GMBs, t_{NF} is typically assessed as the time taken for a GMB property to reach 50% of the initial or the specified value (e.g., Hsuan and Koerner 1998; Rowe et al. 2009; Rowe and Shoaib 2017; Tian et al. 2017; Rowe 2020; Rowe et al. 2020; Francey and Rowe 2022; Abdelaal and Rowe 2023; Zafari et al. 2023). While the same criterion can be applied to BGMs to estimate the loss of mechanical properties, it does not reflect the changes in the bitumen coat that are expected to affect the waterproofing characteristics of the BGM (Samea and Abdelaal 2023a). For this reason, Samea and Abdelaal (2023a) defined the time to nominal failure of the BGM as the time taken either for ε_{max} to reach 50% of the minimum value specified by the manufacturer (Table 1) or for the bitumen coat to reach brittleness and hence loses its waterproofing characteristics. Brittleness of the bitumen coat was observed in Samea and Abdelaal (2023a) when the BGM was exposed to air at different elevated temperatures, and its G^*, δ, and $I_{C=O}$ reached 640 kPa, 20°, and 0.035, respectively. Thus, the t_{NF} of the bitumen coat can be estimated as the time taken for the chemical and rheological properties (i.e., G^*, δ, and $I_{C=O}$) to reach these values signalling the brittleness of the BGM.

Applying Samea and Abdelaal's nominal failure criteria to the current study gave a t_{NF}, based on ε_{max} reaching 50% of the minimum value specified by the manufacturer (i.e., 0.5 x 33 mm), of 2 months at 85°C in PLS pH 11.5 while it was estimated to be reached after 23 months at 70°C

(Figure 10a). In MSW leachate, t_{NF} based on ε_{max} was reached after 10 and 0.8 months at 70 and 85°C, respectively (Figure 10b). For the degradation in the bitumen coat, brittleness was not reached during the 18-month incubation duration reported herein in the PLS pH 11.5 or the MSW leachate even at 85°C. This is due to the relatively slower oxidative degradation of the bitumen in these solutions when compared to immersion in air reported in Samea and Abdelaal (2023a). However, since the degradation in G^*, δ, and $I_{C=O}$ was initiated during the incubation period of 18 months at 55, 70 and 85°C, the best fit lines (Figure 9) were used to assess the degradation rates (Table 3a) and hence predicting the time at which these properties reach the values at brittleness at these temperatures (Table 3b). For example, in PLS pH 11.5 , the time to brittleness based on G^* reaching 640 kPa was estimated as 4.2 years at 85°C (t_{NF} predictions will be discussed in more detail in Section 6). This shows that, at elevated temperatures and in both the PLS pH 11.5 and MSW leachate, the t_{NF} based on mechanical properties was significantly shorter than the t_{NF} based on the time brittleness of the bitumen coat.

6. Estimation of the t_{NF} at field temperatures

The degradation rates (i.e., the slopes of the degradation curves) of the different BGM properties established at 55, 70 and 85°C (Table 3a) were used to estimate the degradation rates and hence the t_{NF} at lower field temperatures using Arrhenius modelling (e.g., Koerner et al. 1992; Rek and Barjaktarović 2002; Rowe and Islam 2009; Naskar et al. 2012; Rowe et al. 2019; Li et al. 2021). Given the multicomponent nature of BGMs, different Arrhenius plots were needed to separately establish the degradation rates for the chemical and rheological properties related to the bituminous component and for the mechanical properties related to the geosynthetic component (i.e., NW-GTX) (Samea and Abdelaal 2023a). The general Arrhenius equation for the mechanical, chemical and rheological properties of the BGM examined can be written as:

$$s = A\, e^{-(Ea / RT)} \quad \text{(Eq 3)}$$

where, s (month^{-1}): degradation rate in a given property of the BGM; A (month^{-1}): collision factor; E_a (J.mol^{-1}): activation energy; R (J.mol^{-1}.K^{-1}): universal gas constant equals 8.314; and T (K): temperature. Taking the natural logarithm of both sides of Eq. (3) gives:

$$\ln(s) = \ln(A) - (E_a/R) \times (1/T) \quad \text{(Eq 4)}$$

To establish the predictions of the degradation rates at lower temperatures from the single-sided experiments, the degradation rates at two elevated temperatures are required. However, using two data points only in the Arrhenius plots may result in highly conservative predictions at lower temperatures, especially if the lowest experimental temperature at which the degradation is obtained is far from the temperatures at which predictions are established (Abdelaal and Rowe 2014a). Thus, three or more temperatures are typically required for better accuracy of the predictions established using Arrhenius plots. Although the degradation rates at 55, 70 and 85°C were established for all the chemical and rheological properties of the BGM (G^*, δ, and $I_{C=O}$), there was limited data at 55°C to confidently establish Arrhenius plots based on δ and $I_{C=O}$ during the 18-month incubation period. Until more data become available to allow better estimates of the rates based on δ and $I_{C=O}$ at 55°C, the Arrhenius plot was established based on G^* only in the current study (Figure 11). This allowed the prediction of the t_{NF} based on the time to brittleness of the bitumen coat at different field temperatures under the single-sided immersion exposure condition (Table 4).

For the mechanical properties of the BGM (i.e., ε_{max}), degradation was only observed at 70 and 85°C as discussed in Section 5, which will affect the accuracy of the Arrhenius predictions of the t_{NF} for the single-sided experiments. However, the ratio of the degradation rate of the

double-sided immersed BGM in a given solution to that in the single-sided experiments at a given temperature (referred to as R_a) can be used to shift the predictions obtained from the double-sided immersion to single-sided exposure (Rowe et al. 2010; 2013). The R_a ratio at 70°C (the only temperature at which degradation to nominal failure was obtained in double-sided and single-sided immersion; Table 3a) was 2.1 and 1.3 in the PLS pH 11.5 and MSW leachate, respectively. These R_a values were used to shift the t_{NF} predictions established from double-sided immersion at temperatures ≤ 40°C. For the experimental temperatures (i.e., 55, 70 and 85°C), the shift factors were applied to the t_{NF} observed experimentally double-sided immersion rather than relying on the predicted values that typically deviate from the experimental estimates (Table 5). While this method provides a preliminary estimate of the t_{NF} under single-sided exposure conditions at lower field temperatures, longer incubation in the Ageing Column experiments is required to establish the Arrhenius plots at three temperatures and hence confirm the accuracy of the estimates reported in the current study. These experiments are running, and the updated results will be reported in future studies.

An alternative approach to predict the t_{NF} for a GMB in a composite liner configuration ($t_{NF(comp)}$) was proposed by Sangam and Rowe (2002). This approach involves a simplified method to infer $t_{NF(comp)}$ (i.e., exposure to the solution from the top surface and unsaturated soil from the bottom) based on the t_{NF} established from double-sided immersion tests of the GMB in air ($t_{NF(air)}$), water ($t_{NF(water)}$), and the solution in contact with the GMB in the field ($t_{NF(solution)}$) viz:

$$t_{NF(comp)} = \frac{t_{NF(Solution)} + t_{NF(unsat)}}{2} \quad \text{(Eq 5)}$$

$$t_{NF(unsat)} = \frac{t_{NF(air)} + t_{NF(water)}}{2} \quad \text{(Eq 6)}$$

Where $t_{NF(unsat)}$ is the time to nominal failure of the GMB when exposed to unsaturated soil (either a GCL or CCL) that can be approximately estimated as the average of $t_{NF(air)}$ and $t_{NF(water)}$.

Given that the BGM examined was immersed in air and water (Samea and Abdelaal 2023a), in PLS pH 11.5 (Abdelaal and Samea 2023), and in MSW leachate (Samea and Abdelaal 2023b), all terms of Equation 5 can be calculated to estimate the $t_{NF(comp)}$ at different field temperatures. This method was used to establish the $t_{NF(comp)}$ of the BGM based on the time of the brittleness of the bitumen coat and the degradation in the mechanical properties.

Tables 4 and 5 compare the calculated $t_{NF(comp)}$ in the PLS pH 11.5 and MSW leachate to the t_{NF} estimates from the double-sided immersion tests (from Abdelaal and Samea 2023 and Samea and Abdelaal 2023b) and the single-sided immersion tests (Ageing Column experiments reported herein) at temperatures between 20 and 85°C. For the time to brittleness, the t_{NF} predictions at different temperatures obtained from the double-sided immersion were similar to those obtained from the single-sided immersion except for some deviations in PLS pH 11.5 at temperatures > 55°C. This can be attributed to the preliminary degradation rates obtained at 55°C in the single-sided immersion during the 18-month incubation that resulted in deviation of the Arrhenius predictions from the experimentally obtained t_{NF} estimates at 70 and 85°C (Table 3b). Thus, longer incubation is needed to improve these predictions, especially at 55°C. For the $t_{NF(comp)}$, the predictions for the PLS pH 11.5 and MSW leachate were consistently lower than the predictions established based on the double-sided and single-sided experiments (Table 4). This can be attributed to the aggressive effect of air exposure on the bitumen degradation (i.e., low values of $t_{NF(air)}$) that was used to approximately calculate $t_{NF(unsat)}$ in Equation 5. Thus, this method underestimates the t_{NF} based on the time to brittleness. However, double-sided immersion in the solution in contact with the BGM in the field presented a good estimate of the t_{NF} related

to the bitumen brittleness in single-sided exposure as long as the PET film is protecting the BGM bottom surface as discussed previously.

For the t_{NF} of the BGM based on the mechanical properties, predictions from the single-sided exposure and Equation 5 ($t_{NF(comp)}$) were greater than those from the double-sided exposure at all temperatures (Table 5). Additionally, the $t_{NF(comp)}$ predictions in MSW leachate were longer than those from the single-sided experiments while in the PLS pH 11.5 , they were shorter than the single-sided t_{NF}. For instance, t_{NF} based on ε_{max} in MSW leachate at 55°C was 4.2 years for the single-sided immersion and the calculated $t_{NF(comp)}$ was 6.3 years while in the PLS pH 11.5 , t_{NF} single-sided immersion was 10.9 years and $t_{NF(comp)}$ was 7.3 years. This shows that the $t_{NF(comp)}$ established using Equation 5 may underestimate or overestimate the predictions for the single-sided field condition depending on the immersion solution being examined. While the $t_{NF(comp)}$ can give an approximate estimate of the BGM longevity based on mechanical properties in a single-sided exposure condition, it should not be used for different BGM materials or different conditions without verification.

7. Practical implications

As previously discussed, the predictions of the t_{NF} presented in Tables 4 and 5 do not represent the time to failure in the field since the stresses on the liner were not simulated in any of the ageing experiments discussed herein. However, the magnitude of the field stresses is expected to define the nominal failure criteria that govern the failure of the BGM in the field. For low-stress applications (e.g., pond, covers) or well-designed liners (e.g., with soil protection above the BGM), if the stresses on the BGM were kept below the values that can induce ruptures in the aged BGM, it is expected that the time to brittleness (i.e., Table 4) will govern the service life of the

BGM in the field. This can be attributed to the potential loss of the waterproofing characteristics of the bitumen coat due to the cracking in the bitumen even at low stresses. In contrast, if the demand on the liner was high enough to induce ruptures in the aged BGM, nominal failure predictions based on the degradation in the mechanical properties are more likely to govern the BGM performance in the field. Thus, the magnitude of the field stresses, and hence the nominal failure criteria (i.e., either the time to brittleness or degradation in the mechanical), can have a significant effect on the estimates of the BGM longevity since the BGM exhibited different degradation rates in its different components. For example, at 30°C in MSW leachate, t_{NF} based on the brittleness in the bitumen coat was 120 years while based on the degradation in ε_{max} it dropped to 24 years only. These results highlight the need to limit the tensile stresses in the field to ensure the longevity of the BGM under field conditions given the fast degradation in its mechanical properties in aqueous solutions such as the MSW leachate or the PLS pH 11.5 examined herein. Additionally, NW-GTX materials with higher resistance to hydrolysis could be used in manufacturing BGMs to increase their t_{NF} related to the degradation in the mechanical properties when exposed to aqueous solutions.

The t_{NF} predictions presented in the current study highlight the effect of two variables on the BGM durability, the exposure media and the liner temperature. While the effect of the exposure media was clear on the degradation of the BGM, the temperature effect in a given solution was far more aggressive on the BGM durability. For instance, the t_{NF} based on ε_{max} predicted at 20°C was 53 years in MSW leachate and 96 years in the PLS pH 11.5 . Increasing the temperature by 35°C (i.e., 55°C), the predictions dropped by one order of magnitude to give 4.2 years in MSW leachate and 10.9 years in the PLS pH 11.5 . As such, thermal protection layers (e.g., soil protection) could be used above the BGM to reduce its temperature during service (to

limit the exposed surface area of the liner to the solution), especially for applications that involve exposure to solutions at elevated temperatures.

8. Conclusions

The effect of single-sided exposure to solutions that represents a closer simulation of the field exposure conditions than the double-sided immersion is examined for a 4.8 mm thick elastomeric BGM at 55, 70, and 85°C. In these custom-designed experiments (Ageing Columns), BGM was exposed from the bitumen coat surface to two different synthetic solutions simulating a high pH mining solution (PLS pH 11.5) and a reduced MSW leachate. The degradation rates from the Ageing Column experiments in the chemical, rheological, and mechanical properties of the BGM were compared to those obtained from previous studies that aged the same BGM in double-sided immersion tests. The following conclusions were reached based on the conditions and the BGM examined:

1. Exposing the BGM from the bitumen coat to the MSW leachate or the PLS pH 11.5 resulted in slower degradation rates in the mechanical properties relative to double-sided immersion. At 70°C, the degradation rate of the elongation at the maximum tensile strength (ε_{max}) was 1.3 and 2.1 times faster in the double-sided than in the single-sided aged samples in MSW leachate and PLS pH 11.5 , respectively.

2. The difference in the degradation rates of the chemical and rheological properties of the bitumen coat between the double-sided and single-sided immersed BGM samples was insignificant. This implies that the extent of oxidative degradation in the bitumen coat in the double-sided exposure is only affected by the solution in contact with the bitumen coat as long as the PET film is protecting the BGM bottom surface. Thus, the time to nominal

failure based on the degradation of the bitumen coat obtained from the double-sided immersion tests can be used as an estimate for the time to nominal failure of the bitumen coat under the single-sided field exposure conditions.

3. The changes in the chemical and rheological properties of the bitumen coat of the samples immersed in the PLS pH 11.5 were greater than those in the MSW leachate. This was attributed to the reduced conditions of the synthetic leachate that resulted in slower oxidative degradation of the bitumen than in the non-reduced PLS pH 11.5 . However, the degradation in the mechanical properties of the BGM was much slower in the PLS pH 11.5 than in MSW leachate due to the presence of the surfactant in the MSW leachate that increased the interaction of its chemical constituents with the NW-GTX.

4. Using Sangam and Rowe's simplified method to infer $t_{NF(comp)}$ based on double-sided immersion experiments underestimated the time to brittleness of the bitumen coat relative to the single-sided exposure established using the Ageing Column experiments but gave an approximate estimation of the time to nominal failure based on ε_{max} established using the Ageing Column experiments.

5. The estimated t_{NF} based on the degradation in mechanical properties was shorter than the t_{NF} estimated based on the brittleness in the bitumen coat in the PLS pH 11.5 and MSW leachate. For example, at 30°C in MSW leachate, t_{NF} based on the brittleness in the bitumen coat was 120 years while based on the degradation in ε_{max}, it dropped to 24 years.

6. Among the different factors that can affect the chemical durability of BGMs, it was found that the BGM temperature had the most significant effect. For example, in MSW leachate,

the predicted t_{NF} based on ε_{max} was 53 years at 20°C, but at 55°C, the predictions dropped by one order of magnitude to give 4.2 years.

7. For high stress applications that involve exposure of the liner to elevated temperatures, a soil protection layer can be used above the BGM liner to limit the tensile strains and to reduce the BGM temperature to increase its time to nominal failure in the field.

The findings of this research are specific to the particular BGM and conditions examined. A geomembrane with high resistance to one solution may not necessarily exhibit the same resistance in different solutions. As such, the predictions presented herein cannot be extrapolated to predict the performance of other BGM products or the same BGM in other solutions without independent verification. Additionally, the experiments presented herein did not simulate the unsaturated soil below the BGM and did not take into account the effects of long-term stress and strain. As a result, the service life of BGMs in the field (i.e., time to rupture) may differ from the predictions presented in this study. However, the results presented herein provided insights into the degradation behaviour of BGMs in the field under single-sided exposure to the solutions relative to the double-sided immersion tests that are commonly used for ageing geomembranes in the laboratory. They also presented preliminary factors that can be used to shift the time nominal failure estimated from the double-sided experiments to the single-sided field conditions.

Acknowledgement

This study was supported by the Natural Science and Engineering Research Council of Canada (NSERC) through the Discovery Grant program to F. B. Abdelaal (RGPIN-2018-04091). The authors would like to acknowledge the funding provided by the Canada Foundation for Innovation (CFI) and the Ontario Ministry of Research and Innovation, which enabled the use of the

necessary equipment. The authors also express their appreciation to Titan Environmental Containment Ltd. for providing the BGM material examined in this study.

Competing Interests Statement

The authors declare there are no competing interests.

Data Availability Statement

Data generated or analyzed during this study are available from the corresponding author upon reasonable request.

References

Abdelaal, F. B. and Rowe, R. K. 2023. "Physical and mechanical performance of a HDPE geomembrane in ten mining solutions with different pHs". *Canadian Geotechnical Journal*. 60(7): 978-993. https://doi.org/10.1139/cgj-2022-0419

Abdelaal, F. B. and Rowe, R. K. 2017. "Effect of high pH found in low-level radioactive waste leachates on the antioxidant depletion of a HDPE geomembrane". *Journal of Hazardous, Toxic, and Radioactive Waste,* 21(1). https://doi.org/10.1061/(ASCE)HZ.2153-5515.0000262

Abdelaal, F., Rowe, R. K. and Brachman, R. 2014a. "Brittle rupture of an aged HPDE geomembrane at local gravel indentations under simulated field conditions". *Geosynthetics International,* 21(1)**,** 1-23. https://doi.org/10.1680/gein.13.00031

Abdelaal, F. B., Rowe, R. K. and Islam, M. Z. 2014b. "Effect of leachate composition on the long-term performance of a HDPE geomembrane". *Geotextiles and Geomembranes,* 42(4)**,** 348-362. https://doi.org/10.1016/j.geotexmem.2014.06.001

Abdelaal, F. B. and Samea, A. 2023. "Chemical durability of elastomeric bituminous geomembranes (BGMs) in heap leach pad application". *Geosynthetics International Journal*, Advance online publication, https://doi.org/10.1680/jgein.22.00333

Addis, P., Andruchow, B., Wislesky, I. 2013. In: Bituminous Geomembrane Failure at a Co-disposal Tailings Storage Facility. Publisher: University of Alberta, Edmonton, Alberta, Canada. *Proceeding Of the 17th International Conference On Tailings And Mine Waste*, Banff, AB, Canada, pp. 457–466. https://doi.org/10.7939/r3-ds53-4h45.

Aguiar-Moya, J. P., Salazar-Delgado, J., García, A., Baldi-Sevilla, A., Bonilla-Mora, V. and Loría-Salazar, L. G. 2017. "Effect of ageing on micromechanical properties of bitumen by means of atomic force microscopy". Road Materials and Pavement Design, 18, 203-215. https://doi.org/10.1080/14680629.2017.1304249

Airey, G. 2003. "Rheological properties of styrene butadiene styrene polymer modified road bitumens". *Fuel,* 82(14)**,** 1709-1719. https://doi.org/10.1016/S0016-2361(03)00146-7

ASTM D4833/D4833M. "Standard Test Method for Index Puncture Resistance of Geomembranes and Related Products". *American Society for Testing and Materials,* West Conshohocken, Pennsylvania, USA.

ASTM D5035. "Standard Test Method for Breaking Force and Elongation of Textile Fabrics (Strip Method)". *American Society for Testing and Materials*, West Conshohocken, Pennsylvania, USA.

ASTM D5199. "Standard Test Method for Measuring the Nominal Thickness of Geosynthetics". *American Society for Testing and Materials*, West Conshohocken, Pennsylvania, USA.

ASTM D5261. "Standard Test Method for Measuring Mass per Unit Area of Geotextiles". *American Society for Testing and Materials*, West Conshohocken, Pennsylvania, USA.

ASTM D7275. "Standard Test Method for Tensile Properties of Bituminous Geomembranes (BGM) ". *American Society for Testing and Materials,* West Conshohocken, Pennsylvania, USA.

ASTM E2602. "Standard Test Methods for the Assignment of the Glass Transition Temperature by Modulated Temperature Differential Scanning Calorimetry". *American Society for Testing and Materials,* West Conshohocken, Pennsylvania, USA.

Bachir, D. S., Dekhli, S. and Mokhtar, K. A. 2016. "Rheological evaluation of ageing properties of SEBS polymer modified bitumens". *Periodica Polytechnica Civil Engineering,* 60(3)**,** 397-404. https://doi.org/10.3311/PPci.7853

Brachman, R., Rowe, R., Arnepalli, D., Dickinson, S., Islam, M. and Sabir, A. 2008. "Development of an apparatus to simulate the ageing of geomembranes under chemical exposure, elevated temperatures and applied stresses". Proceedings GeoAmericas 2008, Cancun, Mexico. 444-451.

Breul, B., Reinson, J., Eldridge, T., G, S. and Harmon, A. 2006. "Bituminous geomembrane in extremely cold conditions". Proceedings of the International Conference of Geosynthetics, Rotterdam, Netherlands, pp. 395-398.

Breul, B., Huru, M. and Palolahti, A. 2008. "Use of bituminous geomembrane (BGM) liner for agnico eagle mine in Kittila (Finland)". Proceedings of the 4th European Geosynthetics Conference. Scotland. Paper, Edinburgh, Scotland.

Cheng, Y., Chai, C., Liang, C., and Chen, Y. 2019. "Mechanical performance of warm-mixed porous asphalt mixture with steel slag and crumb-rubber–SBS modified bitumen for seasonal frozen regions". *Materials*, *12*(6), 857. https://doi.org/10.3390/ma12060857

Cong, P., Wang, J., Luo, W., and Zhang, Y. 2021. "Effects of aging on the properties of SBS modified asphalt binders containing anti-aging agents". *Construction and Building Materials*, 302, 124413. https://doi.org/10.1016/j.conbuildmat.2021.124413

Daly, N. and Breul, B. 2017. "Exceptional Longevity of Bituminous Geomembrane Through Several Decades of Practice". Proceedings of 70th Canadian Geotechnical Conference, 2017, Ottawa, Canada. Publisher: Canadian Geotechnical Society,Surrey, BC, Canada.

Daly, N., Aguirre, T., Breul, B., Breul, B. and Barfett, B. 2018. "Bituminous geomembranes (BGM) for heap leach pads and dumps for solid wastes in mine construction". Proceedings of the 71st Canadian Geotechnical Conference, Edmonton, AB, Canada.

Durrieu, F., Farcas, F. and Mouillet, V. 2007. "The influence of UV aging of a Styrene/Butadiene/Styrene modified bitumen: comparison between laboratory and on site aging". *Fuel,* 86(10-11)**,** 1446-1451. https://doi.org/10.1016/j.fuel.2006.11.024

Ewais, A. M. R., Rowe, R. K. and Scheirs, J. 2014. "Degradation behaviour of HDPE geomembranes with high and low initial high-pressure oxidative induction time". *Geotextiles and Geomembranes,* 42(2)**,** 111-126. https://doi.org/10.1016/j.geotexmem.2014.01.004

Feng, B., Wang, H., Li, S., Ji, K., Li, L. and Xiong, R. 2022. "The durability of asphalt mixture with the action of salt erosion: A review". *Construction and Building Materials,* 315**,** 125749. https://doi.org/10.1016/j.conbuildmat.2021.125749

Francey, W. and Rowe, R. K. 2022. "Long-term stress crack eesistance of HDPE fusion seams aged at 85°C in synthetic leachate". *Canadian Geotechnical Journal*, 60(3), 251-268 https://doi.org/10.1139/cgj-2022-0159

Frolov, I. N., Okhotnikova, E. S., Ziganshin, M. A., Yusupova, T. N. and Firsin, A. A. 2019. "The study of bitumen by differential scanning calorimetry: The interpretation of thermal effects". *Petroleum Science and Technology,* 37(4), 417-424. https://doi.org/10.1080/10916466.2018.1550499

Gao, Y., Gu, F. and Zhao, Y. 2013. "Thermal oxidative aging characterization of SBS modified asphalt". *Journal of Wuhan University of Technology-Mater. Sci. Ed.,* 28, 88-91. https://doi.org/10.1007/s11595-013-0646-0

Gulec, S., Edil, T. and Benson, C. 2004. "Effect of acidic mine drainage on the polymer properties of an HDPE geomembrane". *Geosynthetics International,* 11(2), 60-72. https://doi.org/10.1680/gein.2004.11.2.60

Hrapovic, L., 2001. "Laboratory study of intrinsic degradation of organic pollutants in compacted clayey soil doctoral thesis". Civil Engineering Department, University of Western, Ontario, Canada.

Hsuan, Y. and Koerner, R. 1998. "Antioxidant depletion lifetime in high density polyethylene geomembranes". *Journal of Geotechnical and Geoenvironmental Engineering,* 124(6), 532-541. https://doi.org/10.1061/(ASCE)1090-0241(1998)124:6(532)

Jeon, H.-Y., Bouazza, A. and Lee, K.-Y. 2008. "Depletion of antioxidants from an HDPE geomembrane upon exposure to acidic and alkaline solutions". *Polymer Testing,* 27(4), 434-440. https://doi.org/10.1016/j.polymertesting.2008.01.003

Kaya, D., Topal, A., Gupta, J. and Mcnally, T. 2020. "Aging effects on the composition and thermal properties of styrene-butadiene-styrene (SBS) modified bitumen". *Construction and Building Materials,* 235. https://doi.org/10.1016/j.conbuildmat.2019.117450

Keys, H., 2021. Townsville undertakes Australia first geomembrane landfill rehabilitation [Online]. Waste Management Review. Available: https://wastemanagementreview.com.au/townsville-undertakes-australia-first-geomembrane-landfill-rehabilitation/ (Accessed 1 December 2022)

Koerner, R. M., Lord, A. E. and Hsuan, Y. H. 1992. "Arrhenius modeling to predict geosynthetic degradation". *Geotextiles and Geomembranes,* 11(2)**,** 151-183. https://doi.org/10.1016/0266-1144(92)90042-9

Lamontagne, J., Dumas, P., Mouillet, V. and Kister, J. 2001. "Comparison by Fourier transform infrared (FTIR) spectroscopy of different ageing techniques: application to road bitumens". *Fuel,* 80(4)**,** 483-488. https://doi.org/10.1016/S0016-2361(00)00121-6

Lazaro, J. and Breul, B. 2014. "Bituminous geomembrane in heap leach pads". Proceedings of Heap Leach Solutions, Lima, Peru. InfoMine Inc., Canada, pp. 291-303.

Li, W., Xu, Y., Huang, Q., Liu, Y. and Liu, J. 2021. "Antioxidant depletion patterns of high-density polyethylene geomembranes in landfills under different exposure conditions". *Waste Management,* 121**,** 365-372. https://doi.org/10.1016/j.wasman.2020.12.025

Liu, K., Xu, G., Voyer, R. 2003. "Durability and cold temperature performance of SBS-modified bituminous roofing membranes". In: Wallace, T.J. (Ed.), Roofing Research And Standards Development: 5th Volume. ASTM STP 145, W. J. Rossiter. ASTM International, West Conshohocken, PA. https://doi.org/10.1520/stp11453s.

Lu, X. and Isacsson, U. 2002. "Effect of ageing on bitumen chemistry and rheology". *Construction and Building Materials,* 16(1)**,** 15-22. https://doi.org/10.1016/S0950-0618(01)00033-2

Lu, X., Talon, Y. and Redelius, P. 2008. "Ageing of bituminous binders - laboratory tests and field data". Proceedings of the 4th Eurasphalt & Eurobitume Congress, European Asphalt Pavement Association (EAPA), Copenhagen. Denmark, pp. 21-23.

Lupo, J. F. 2010. "Liner system design for heap leach pads". *Geotextiles and Geomembranes,* 28(2)**,** 163-173. https://doi.org/10.1016/j.geotexmem.2009.10.006

Mark, J., Ngai, K., Graessley, W., Mandelkern, L., Samulski, E., Koenig, J. and Wignall, G. 2004. "The glass transition and the glassy state". *Physical Properties of Polymers*. 3 ed. Cambridge: Cambridge University Press, pp. 72-152.

Morsy, M. S., Rowe, R. K., and Abdelaal, F. B. 2021. "Longevity of 12 geomembranes in chlorinated water". *Canadian Geotechnical Journal*, *58*(4), 479-495. https://doi.org/10.1139/cgj-2019-0520

Mouillet, V., Farcas, F., Chailleux, E. 2011. "Physico-chemical techniques for analysing the ageing of polymer modified bitumen". In: Chapter 12, polymer modified bitumen: properties and characterisation. Tony McNally, Woodhead Publishing Limited, Cambridge, UK, pp. 366–395. https://doi.org/10.1533/9780857093721.2.366.

Naskar, M., Reddy, K. S., Chaki, T. K., Divya, M. K. and Deshpande, A. P. 2012. "Effect of ageing on different modified bituminous binders: comparison between RTFOT and radiation ageing". *Materials and Structures,* 46**,** 1227-1241. https://doi.org/10.1617/s11527-012-9966-3

Omairey, E. L., Zhang, Y., Gu, F., Ma, T., Hu, P. and Luo, R. 2020. "Rheological and fatigue characterisation of bitumen modified by anti-ageing compounds". *Construction and Building Materials,* 265**,** 120307. https://doi.org/10.1016/j.conbuildmat.2020.120307

Peggs, I. 2008. "Prefabricated bituminous geomembrane: a candidate for exposed geomembrane caps for landfill closures". Proceedings of the first Pan American Geosynthetics Conference and Exhibition, Cancun, Mexico. Industrial Fabrics Association International (IFAI), USA, 191-197.

Puello, J., Afanasjeva, N. and Alvarez, M. 2013. "Thermal properties and chemical composition of bituminous materials exposed to accelerated ageing". *Road Materials and Pavement Design*, 14(2), 278-288. https://doi.org/10.1080/14680629.2013.785799

Rek, V. and Barjaktarović, Z. M. 2002. "Dynamic mechanical behavior of polymer modified bitumen". *Materials Research Innovations,* 6**,** 39-43. https://doi.org/10.1007/s10019-002-0159-5

Richardson, D. and Wingrove, P. 2021. SRWRA Western Side Liner, Adelaide [PowerPoint slides]. https://www.wmrr.asn.au/common/Uploaded%20files/ALTS/2021/Don%20Richardson.pdf. (Accessed 1 December 2022)

Rowe, R. K. 2020. "Protecting the Environment with Geosynthetics: 53rd Karl Terzaghi Lecture". *Journal of Geotechnical and Geoenvironmental Engineering,* 146(9)**,** 04020081. doi:10.1061/(ASCE)GT.1943-5606.0002239

Rowe, R., Abdelaal, F. and Brachman, R. 2013. "Antioxidant depletion of HDPE geomembrane with sand protection layer". *Geosynthetics International,* 20(2)**,** 73-89. https://doi.org/10.1680/gein.13.00003

Rowe, R. K. 2005. "Long-term performance of contaminant barrier systems". *Géotechnique,* 55**,** 631-678. https://doi.org/10.1680/geot.2005.55.9.631

Rowe, R. K., Abdelaal, F., Zafari, M., Morsy, M. and Priyanto, D. 2020. "An approach to high-density polyethylene (HDPE) geomembrane selection for challenging design requirements". *Canadian Geotechnical Journal,* 57**,** 1550-1565. https://doi.org/10.1139/cgj-2019-0572

Rowe, R. K. and Islam, M. Z. 2009. "Impact of landfill liner time–temperature history on the service life of HDPE geomembranes". *Waste Management,* 29(10)**,** 2689-2699. https://doi-org.proxy.queensu.ca/10.1016/j.wasman.2009.05.010

Rowe, R. K., Islam, M., Brachman, R., Arnepalli, D. and Ewais, A. R. 2010. "Antioxidant depletion from a high density polyethylene geomembrane under simulated landfill conditions". *Journal of Geotechnical and Geoenvironmental Engineering,* 136(7)**,** 930-939. https://doi.org/10.1061/(ASCE)GT.1943-5606.0000302

Rowe, R. K., Morsy, M. and Ewais, A. 2019. "Representative stress crack resistance of polyolefin geomembranes used in waste management". *Waste Management,* 100**,** 18-27. https://doi.org/10.1016/j.wasman.2019.08.028

Rowe, R. K., Quigley, R. M., Brachman, R. W. and Booker, J. R. 2004. *Barrier systems for waste disposal facilities,* London, Taylor & Francis Books Ltd. (E & FN Spon).

Rowe, R. K. and Rimal, S. 2008. "Depletion of antioxidants from a HDPE geomembrane in a composite liner". *Journal of Geotechnical and Geoenvironmental Engineering,* 134(1)**,** 68-78. https://doi.org/10.1061/(ASCE)1090-0241(2008)134:1(68)

Rowe, R. K., Rimal, S. and Sangam, H. 2009. "Ageing of HDPE geomembrane exposed to air, water and leachate at different temperatures". *Geotextiles and Geomembranes,* 27(2)**,** 137-151. https://doi.org/10.1016/j.geotexmem.2008.09.007

Rowe, R. K. and Somuah, M. 2023. "Effects of perfluoroalkyl substances (PFAS) on antioxidant depletion from a high-density polyethylene geomembrane". *Journal of Environmental Management,* 328**,** 116979. https://doi.org/10.1016/j.jenvman.2022.116979

Rowe, R. K. and Shoaib, M. 2017. "Long-term performance of high-density polyethylene (HDPE) geomembrane seams in municipal solid waste (MSW) leachate". *Canadian Geotechnical Journal,* 54(12)**,** 1623-1636. https://doi.org/10.1139/cgj-2017-0049

Samea, A. and Abdelaal, F. B. 2023a. "Effect of elevated temperatures on the degradation behaviour of elastomeric bituminous geomembranes". *Geotextiles and Geomembranes,* 51**,** 219-232. https://doi.org/10.1016/j.geotexmem.2022.10.010

Samea, A. and Abdelaal, F. B. 2023b. "Durability of two bituminous geomembranes (BGMs) with different thicknesses in MSW synthetic leachate". Waste Management Journal, 165, 179-188. https://doi.org/10.1016/j.wasman.2023.04.031

Sangam, H. P. and Rowe, R. K. 2002. "Effects of exposure conditions on the depletion of antioxidants from high-density polyethylene (HDPE) geomembranes". *Canadian Geotechnical Journal,* 39(6)**,** 1221-1230. https://doi.org/10.1139/t02-074

Scheirs, J. 2009. *A guide to polymeric geomembranes: a practical approach,* West Sussex, United Kingdom, John Wiley & Sons.

Su, Y., Tang, S., Cai, M., Nie, Y., Hu, B., Wu, S. and Cheng, C. 2023. "Thermal oxidative aging mechanism of lignin modified bitumen". *Construction and Building Materials,* 363**,** 129863. https://doi.org/10.1016/j.conbuildmat.2022.129863

Tian, K., Tinjum, J. M., Benson, C. H. and Edil, T. B. 2014. "Antioxidant depletion in HDPE geomembranes exposed to low-level radioactive waste leachate". *Geo-Congress 2014:*

Geo-characterization and Modeling for Sustainability, 1816-1825. https://doi.org/10.1061/9780784413272.178

Tian, K., Benson, C. H., Tinjum, J. M. and Edil, T. B. 2017. "Antioxidant depletion and service life prediction for HDPE geomembranes exposed to low-level radioactive waste leachate". *Journal of Geotechnical and Geoenvironmental Engineering,* 143(6), 04017011. https://doi.org/10.1061/(ASCE)GT.1943-5606.0001643

Touze-Foltz, N. and Farcas, F. 2017. "Long-term performance and binder chemical structure evolution of elastomeric bituminous geomembranes". *Geotextiles and Geomembranes,* 45(2), 121-130. https://doi.org/10.1016/j.geotexmem.2017.01.003

Vahidi, S., Hsuan, G. and Elsafty, A. 2020. "Predicting the depletion of antioxidants in high density polyethylene (HDPE) under sunlight using the reciprocity law". *Geotextiles and Geomembranes,* 48(2), 170-175. https://doi.org/10.1016/j.geotexmem.2019.11.009

Wang, D., Liu, Q., Yang, Q., Tovar, C., Tan, Y. and Oeser, M. 2019. "Thermal oxidative and ultraviolet ageing behaviour of nano-montmorillonite modified bitumen". *Road Materials and Pavement Design,* 22, 121-139. https://doi.org/10.1080/14680629.2019.1619619

Yang, Z., Zhang, X., Zhang, Z., Zou, B., Zhu, Z., Lu, G., Xu, W., Yu, J. and Yu, H. 2018. "Effect of aging on chemical and rheological properties of bitumen". *Polymers,* 10(12), 1345. https://doi.org/10.3390/polym10121345

Yu, H., Bai, X., Qian, G., Wei, H., Gong, X., Jin, J., and Li, Z. 2019. "Impact of ultraviolet radiation on the aging properties of SBS-modified asphalt binders". *Polymers,* 11(7), 1111. https://doi.org/10.3390/polym11071111

Yu, X., Zaumanis, M., Dos Santos, S. and Poulikakos, L. D. 2014. "Rheological, microscopic, and chemical characterization of the rejuvenating effect on asphalt binders". *Fuel,* 135**,** 162-171. https://doi.org/10.1016/j.fuel.2014.06.038

Zafari, M., Abdelaal, F. and Rowe, R. K. 2023. "Degradation Behavior of Two Multilayered Textured White HDPE Geomembranes and Their Smooth Edges". *Journal of Geotechnical and Geoenvironmental Engineering,* 149(5)**,** 04023020. https://doi.org/10.1061/JGGEFK.GTENG-11101

Zhang, X., Chen, H. and Hoff, I. 2021. "The mutual effect and reaction mechanism of bitumen and de-icing salt solution". *Construction and Building Materials,* 302**,** 124213. https://doi.org/10.1016/j.conbuildmat.2021.124213

Zeng, W., Wu, S., Wen, J. and Chen, Z. 2015. "The temperature effects in aging index of asphalt during UV aging process". *Construction and Building Materials,* 93**,** 1125-1131. https://doi.org/10.1016/j.conbuildmat.2015.05.022

Zhu, J., Birgisson, B. and Kringos, N. 2014. "Polymer modification of bitumen: Advances and challenges". *European Polymer Journal,* 54**,** 18-38. https://doi.org/10.1016/j.eurpolymj.2014.02.005

Table 1. Initial properties of the examined materials (mean ± standard deviation)

Property[a]	Method	BGM	NW-GTX*
Designator	--	TERANAP 531 TP 4M	--
Nominal Thickness (mm)	ASTM D5199	4.8± 0.120 (4.6)	1.1 ± 0.128
Glass Mat. Reinforcement (g/m^2)	--	50[c]	--
Mass Per Unit Area of the Nonwoven Geotextile Reinforcement (g/m^2)	ASTM D5261	275[c]	275
Mass Per Unit Area of the BGM (g/m^2)	ASTM D5261	5410[c]	--
Machine Direction Maximum Tensile Strength (kN/m)	ASTM D7275	33.1 ± 0.422 (25.5)	--
	ASTM D5035	--	13.4 ± 1.33
Machine Direction Elongation at Maximum Tensile Strength (mm)	ASTM D7275	51 ± 1.8 (33)	--
	ASTM D5035	--	48 ± 3.7
Cross Machine Maximum Tensile Strength (kN/m)	ASTM D7275	29.5 ± 0.887 (23)	--
	ASTM D5035	--	10.5 ± 0.866
Cross Machine Elongation at Maximum Tensile Strength (mm)	ASTM D7275	52 ± 1.5 (35.7)	--
	ASTM D5035	--	55 ±1.2
Peak Puncture Resistance (N)	ASTM D4833	690 ± 41.91 (555)	627 ± 62.37
Puncture Elongation at Peak Puncture Resistance (mm)	ASTM D4833	14.35 ± 0.933	16.79 ± 0.665
Glass Transition Temperature of Bitumen Tack Coat (°C)	ASTM E2602	-24.2 ± 1.48	82.86 ± 2.27
Complex Shear Modulus (kPa)	--	112 ± 7.38	--
Phase Angle (°)	--	43 ± 0.53	--
Carbonyl Index	--	2.38e-3 ± 5.23e-4	--
SBS Index	--	0.014 ± 7.89e-4	--

*The NW-GTX used in manufacturing the BGM was provided separately by the BGM manufacturer

[a] 10 replicates were examined for each property.

[b] Values in parentheses show the minimum specified value by the manufacturer for this BGM.

[c] Values from the manufacturer datasheet.

Table 2. Chemical composition of the different solutions used in this study (mg/l except for pH, Eh and Surfactant)

Analyte[a]	PLS[b]	MSW leachate[c]
Designator	**PLS3**	**L3**
Nominal pH	11.5	7.1
Eh	~+115 (mV)	~ -120 (mV)
Aluminum	<1.0	<1.0
Ammonium[d]	--	555
Arsenic	0.9	--
Barium	0.1	--
Cadmium	<0.025	--
Calcium	0.64	732
Carbamide	--	695
Copper	9	<0.2
Cobalt	0.03	0.03
Iron	<0.05	0.41
Magnesium	2.8	395
Manganese	--	<0.05
Molybdenum	0.56	<0.05
Nickel	<0.3	<0.3
Lead	<0.03	--
Lithium	<0.05	--
Phosphorus	--	5.7
Potassium	181	316
Silver	0.3	--
Sodium	138	814
Sulfur	--	446
Zinc	0.02	0.014
Chloride	<0.5	2370
Hydroxides	9440	--
Oxides	0.59	--
Sulphate	300	1330
Carbonate[d]	--	140
Bicarbonate[d]	--	4260
Nitrate	--	<12.5
Hydrogen phosphate	--	<25
Surfactant (IGEPAL® CA720)	--	5 ml/l

[a] Dissolved metal ions were analyzed using an inductively coupled plasma-mass spectrometer (ICP-MS), while the anions were analyzed using Ion chromatography (IC).
[b] Values after Abdelaal and Rowe (2017).
[c] Values after Abdelaal et al. (2014b).
[d] Calculated values since no tests were performed to detect these ions.

Table 3a. Degradation rates of the BGM samples aged in Ageing Columns

Solution	Property	Degradation rates at different temperatures (month^{-1})					
		55°C		70°C		85°C	
		Double-sided immersion[a]	Single-sided immersion	Double-sided immersion[a]	Single-sided immersion	Double-sided immersion[a]	Single-sided immersion
PLS pH 11.5	ε_{max}	0.55	NR	3.2	1.5	--	14
	G*	4.5	4.3	7	6.9	--	10.5
	δ	0.34	0.32	0.72	0.73	--	1.0
	$I_{C=O}$	0.00032	0.00038	0.00065	0.00067	--	0.0012
MSW leachate	ε_{max}	0.90	NR	4.50	3.4	--	34
	G*	1.5	1.4	3.80	3.9	--	5
	δ	0.17	0.17	0.45	0.42	--	0.60
	$I_{C=O}$	0.0002	0.0002	0.00040	0.00042	--	0.0010

Table 3b. Experimentally estimated times to nominal failure (t_{NF}) of the BGM samples aged in Ageing Columns

Solution	Property	Estimated t_{NF} (years)					
		55°C		70°C		85°C	
		Double-sided immersion[a]	Single-sided immersion	Double-sided immersion[a]	Single-sided immersion	Double-sided immersion[a]	Single-sided immersion
PLS pH 11.5	ε_{max}	5.2	NR	0.9	1.9	--	0.2
	G*	9.8	10.2	6.3	6.4	--	4.2
	δ	5.5	5.9	2.6	2.6	--	1.9
	$I_{C=O}$	8.5	7.1	4.2	4.5	--	2.3
MSW leachate	ε_{max}	3.2	NR	0.65	0.85	--	0.08
	G*	29.3	31.4	11.6	11.3	--	8.8
	δ	11.1	11.1	4.2	4.2	--	3.1
	$I_{C=O}$	13.6	13.6	6.8	6.8	--	2.7

NR= Degradation in properties was not reached during the current study.
Immersion tests were not conducted at 85°C in the double-sided immersion tests
[a] Values from Abdelaal and Samea (2023) for the PLS and Samea and Abdelaal (2023b) for the MSW leachate.

Table 4. Comparison between the predicted times to nominal failure (t_{NF}) of the BGM in the PLS and MSW leachate based on the time of brittleness in the bitumen coat

T (°C)	t_{NF} (in years) based on the time of brittleness based on G^* of brittleness point (640 kPa)					
	MSW leachate			PLS pH 11.5		
	Double-sided immersion[a]	Single-sided immersion[c]	Composite liner method[d]	Double-sided immersion[b]	Single-sided immersion [c]	Composite liner method[d]
20	225	240	170	130	120	120
30	115	120	83	65	66	58
40	63	66	45	35	38	31
55	27	28	19	12	17	11
70	12	13	8.4	5.5	8.5	5.1
85	6.1	6.2	4.1	2.5	4.4	2.4

[a] Predicted values from Samea and Abdelaal (2023b).
[b] Predicted values from Abdelaal and Samea (2023).
[c]Single-sided immersion predictions are based on Arrhenius modelling (Figure 11).
[d] $t_{NF(comp)}$ calculated using Equation 5 based on the simplified method proposed by Sangam and Rowe (2002).

Table 5. Comparison between the predicted times to nominal failure (t_{NF}) of the BGM in the PLS and MSW leachate based on mechanical properties

T (°C)	t_{NF} (in years) based on ε_{max} reaching 50% of the minimum values specified by the manufacturer					
	MSW leachate			PLS pH 11.5		
	Double-sided immersion[a]	Single-sided immersion[b]	Composite liner method[c]	Double-sided immersion[d]	Single-sided immersion[b]	Composite liner method[c]
20	40	53	74	45	96	76
30	18	24	34	20	43	35
40	8.4	11	17	9.7	21	17
55	3.2	4.2	6.3	5.2	10.9	7.3
70	0.65	0.85	1.6	0.9	1.9	1.7
85	NA	0.08	NA	NA	0.2	NA

NA= Double-sided immersion tests from Abdelaal and Samea (2023) and Samea and Abdelaal (2023b) were not conducted at 85°C.

[a] Data ≤ 40°C is predicted using the Arrhenius equation in Samea and Abdelaal (2023b) while at temperatures > 40°C the t_{NF} was established experimentally.

[b] Predictions are based on the shift factors (R_a = 1.3 for MSW leachate and 2.1 for the PLS) established from the ratio of degradation in double-sided immersion to that from single-sided immersion at 70°C. t_{NF} estimates at 85°C are from the experimental data of the single-sided immersion tests (Figure 10).

[c] $t_{NF(comp)}$ calculated using Equation 5 based on the simplified method proposed by Sangam and Rowe (2002).

[d] Data ≤ 40°C is predicted using the Arrhenius equation in Abdelaal and Samea (2023) while at temperatures > 40°C the t_{NF} was established experimentally.

Figure Captions

Figure 1. Ageing Column configuration used in the current study: (a) Vertical cross-section showing a typical test configuration (not to scale); (b) Photograph of an assembled column.

Figure 2. Variation in glass transition temperature (T_g) with incubation time at 70°C for double and single-sided immersion in (a) PLS pH 11.5; (b) MSW leachate. The double-sided immersion data and their fitting curves are from Abdelaal and Samea (2023) and Samea and Abdelaal (2023b).
Unless otherwise noted, the data points presented in all the figures represent the mean value, while the error bars represent the ±1 standard deviation of the data.

Figure 3. Variation of the rheological properties with incubation time at 70°C for double and single-sided immersion in PLS pH 11.5 and MSW leachate: (a) complex shear modulus (G^*) in PLS pH 11.5; (b) phase angle (δ) in PLS pH 11.5; (c) G^* in MSW leachate; (d) δ in MSW leachate. The double-sided immersion data and their fitting curves are from Abdelaal and Samea (2023) and Samea and Abdelaal (2023b).

Figure 4. Variation with the incubation time at 70°C for double and single-sided immersion in PLS pH 11.5 and MSW leachate of (a) Carbonyl index ($I_{C=O}$) in PLS pH 11.5; (b) Butadiene index (I_{SBS}) in PLS pH 11.5; (c) $I_{C=O}$ in MSW leachate; (d) I_{SBS} in MSW leachate. The double-sided immersion data and their fitting curves are from Abdelaal and Samea (2023) and Samea and Abdelaal (2023b).

Figure 5. Variation of the tensile properties in the machine direction with incubation time at 70°C for double and single-sided immersion in PLS pH 11.5 and MSW leachate (a) maximum tensile stress (σ_{max}) in PLS pH 11.5; (b) elongation at maximum tensile strength (ε_{max}) in PLS pH 11.5; (c) σ_{max} in MSW leachate; (d) ε_{max} in MSW leachate. The double-sided immersion data and their fitting curves are from Abdelaal and Samea (2023) and Samea and Abdelaal (2023b).

Figure 6. Variation of the puncture properties with incubation time at 70°C for double and single-sided immersion in PLS pH 11.5 and MSW leachate (a) peak puncture force in PLS pH 11.5; (b) elongation at peak puncture force in PLS pH 11.5; (c) peak puncture force MSW leachate; (d) elongation at peak puncture force in MSW leachate. The double-sided immersion data and their fitting curves are from Abdelaal and Samea (2023) and Samea and Abdelaal (2023b).

Figure 7. Variation of the different normalized properties (aged values/initial values) of the BGM with incubation time obtained from the single-sided immersion at 70oC in (a) PLS pH 11.5; (b) MSW leachate.

Figure 8. Variation in the normalized (aged values/initial values) elongation at maximum tensile strength (ε_{max}) with incubation time of the double-sided immersed BGM (with sealed edges), single-sided immersed BGM, and the NW-GTX samples at 55°C in (a) PLS pH 11.5; (b) MSW leachate. The double-side immersion data and their fitting curves are from Abdelaal and Samea (2023) and Samea and Abdelaal (2023b).

Figure 9. Variation of the complex shear modulus (G^*) with the incubation time of the BGM at different temperatures in (a) PLS pH 11.5; (b) MSW leachate.

Figure 10. Variation of the elongation at maximum tensile strength (ε_{max}) with the incubation time of the BGM at different temperatures in (a) PLS pH 11.5; (b) MSW leachate.

Figure 11. Arrhenius plots of the complex shear modulus (G^*) for the single-sided BGM samples immersed in PLS pH 11.5 and MSW leachate.

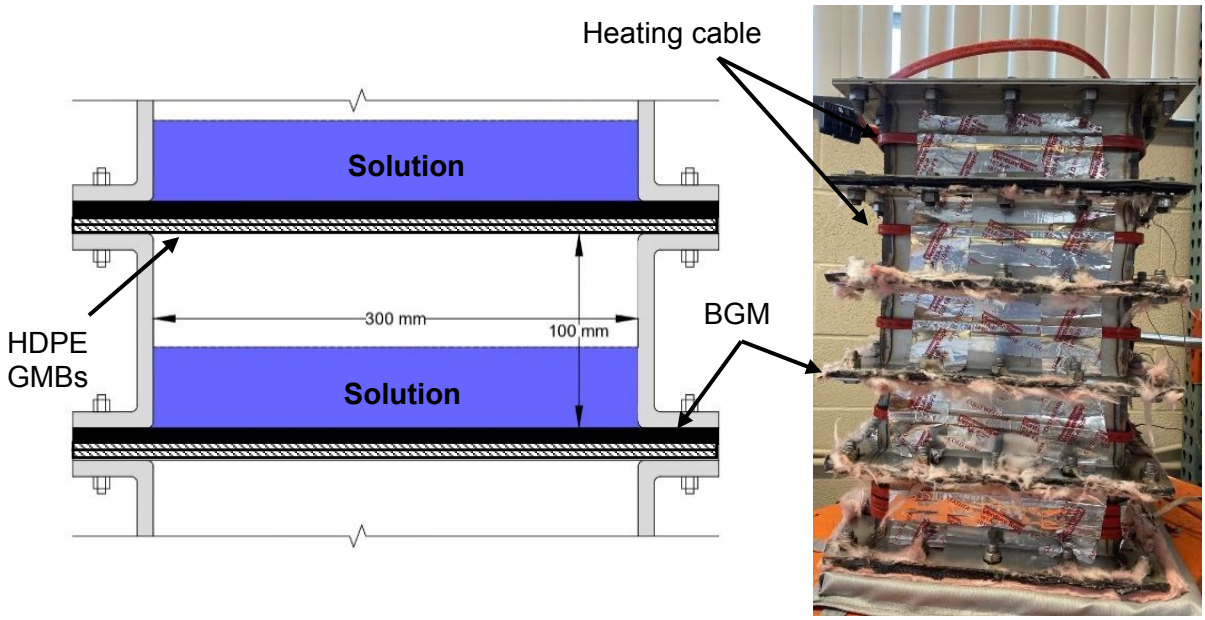

Figure 1. Ageing Column configuration used in the current study: (a) Vertical cross-section showing a typical test configuration (not to scale); (b) Photograph of an assembled column.

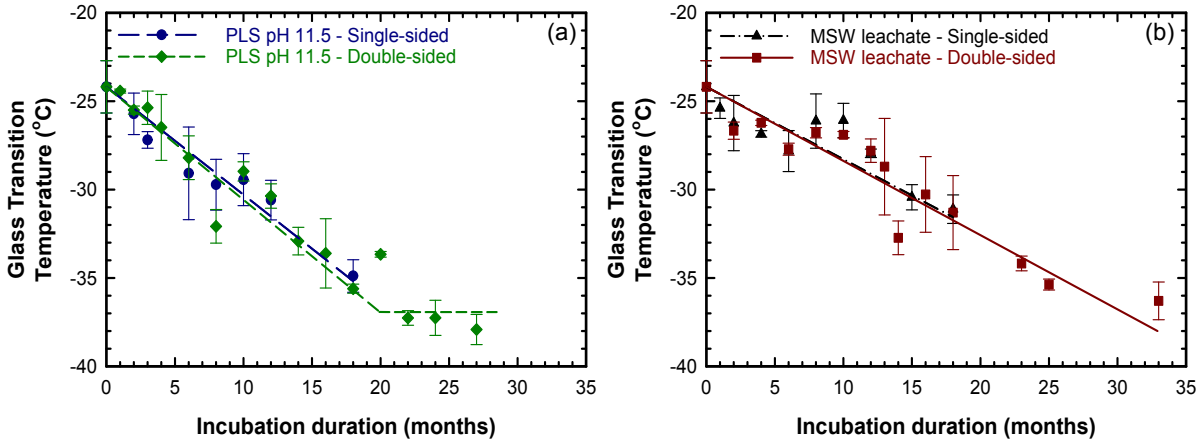

Figure 2. Variation in glass transition temperature (T_g) with incubation time at 70°C for double and single-sided immersion in (a) PLS pH 11.5; (b) MSW leachate. The double-sided immersion data and their fitting curves are from Abdelaal and Samea (2023) and Samea and Abdelaal (2023b).

Unless otherwise noted, the data points presented in all the figures represent the mean value, while the error bars represent the ±1 standard deviation of the data.

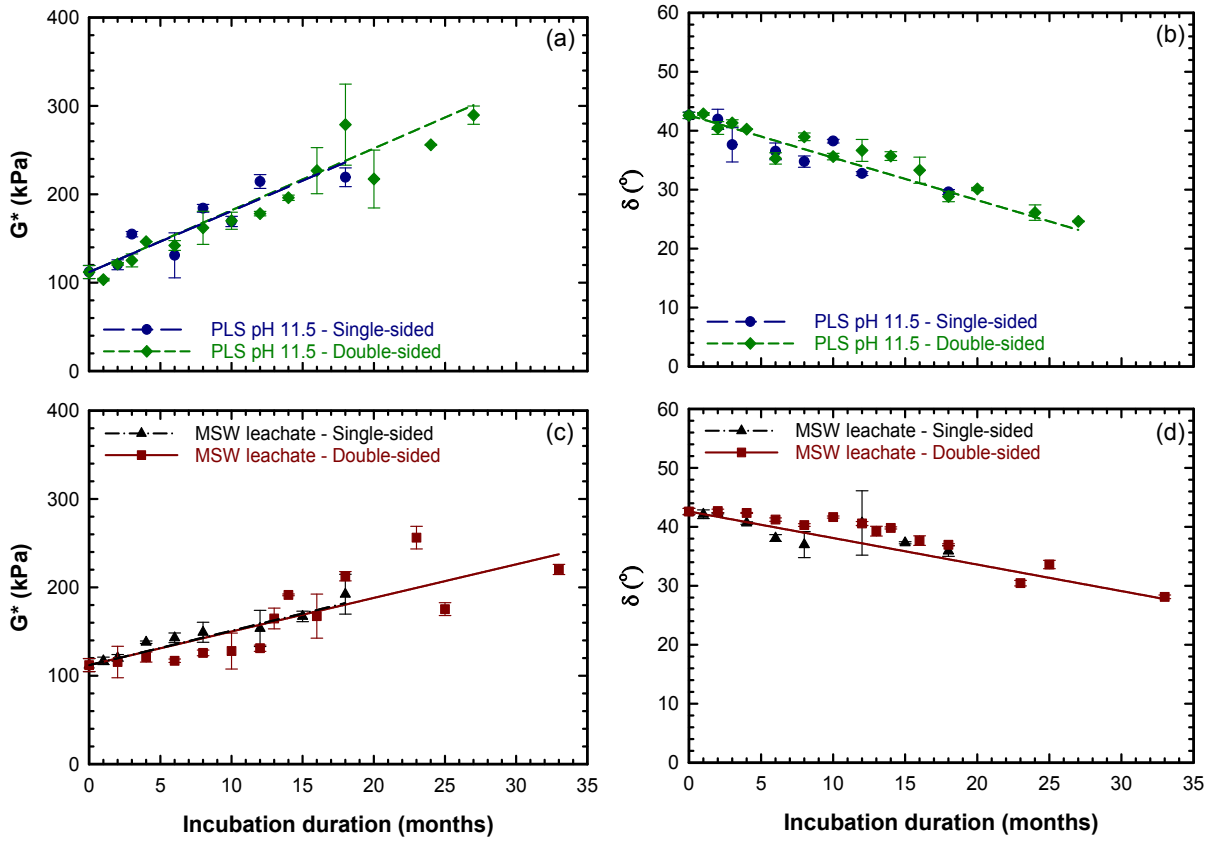

Figure 3. Variation of the rheological properties with incubation time at 70°C for double and single-sided immersion in PLS pH 11.5 and MSW leachate: (a) complex shear modulus (G^*) in PLS pH 11.5; (b) phase angle (δ) in PLS pH 11.5; (c) G^* in MSW leachate; (d) δ in MSW leachate. The double-sided immersion data and their fitting curves are from Abdelaal and Samea (2023) and Samea and Abdelaal (2023b).

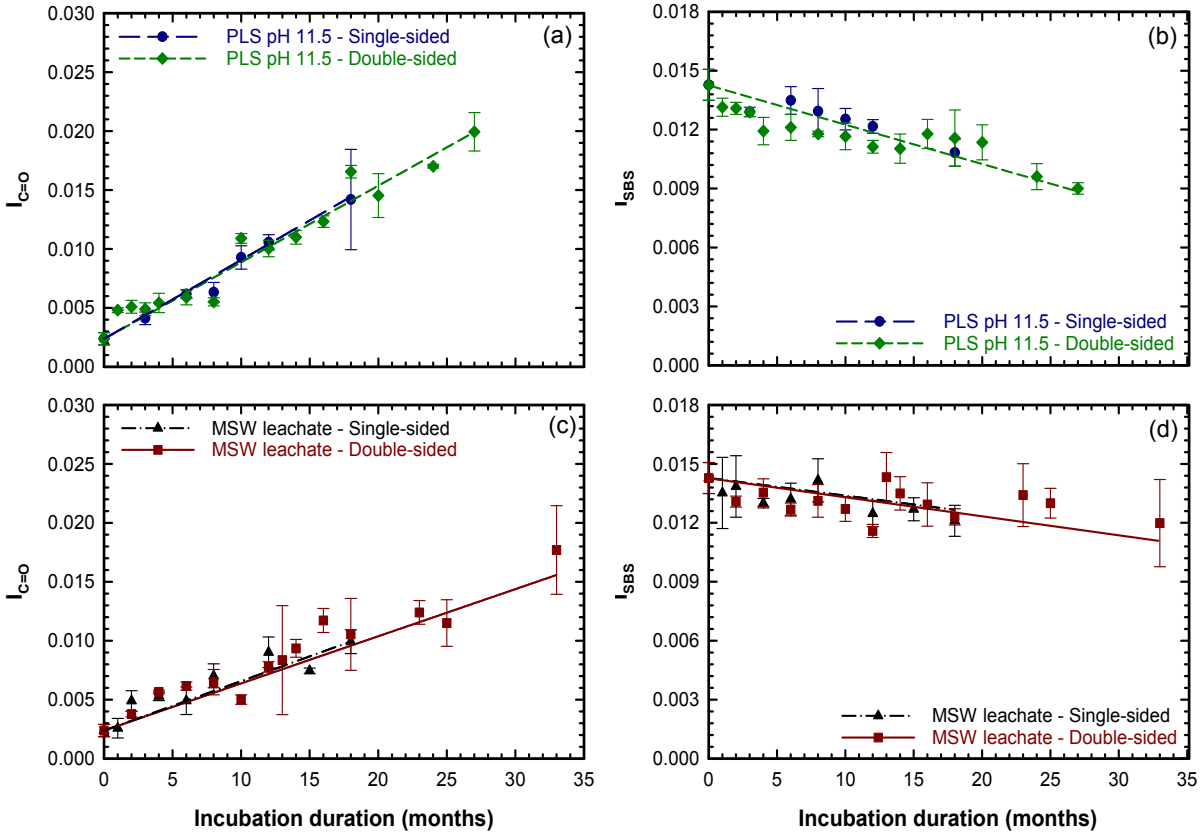

Figure 4. Variation with the incubation time at 70°C for double and single-sided immersion in PLS pH 11.5 and MSW leachate of (a) Carbonyl index ($I_{C=O}$) in PLS pH 11.5; (b) Butadiene index (I_{SBS}) in PLS pH 11.5; (c) $I_{C=O}$ in MSW leachate; (d) I_{SBS} in MSW leachate. The double-sided immersion data and their fitting curves are from Abdelaal and Samea (2023) and Samea and Abdelaal (2023b).

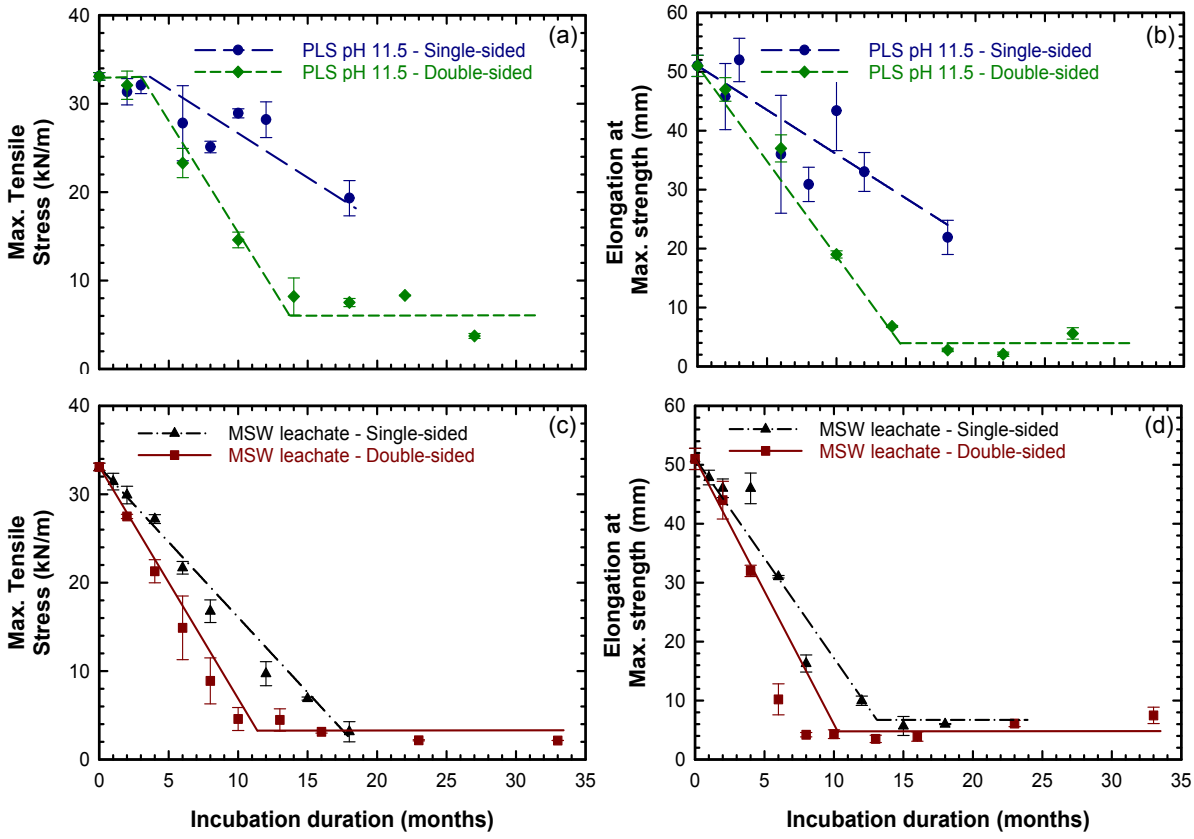

Figure 5. Variation of the tensile properties in the machine direction with incubation time at 70°C for double and single-sided immersion in PLS pH 11.5 and MSW leachate (a) maximum tensile stress (σ_{max}) in PLS pH 11.5; (b) elongation at maximum tensile strength (ε_{max}) in PLS pH 11.5; (c) σ_{max} in MSW leachate; (d) ε_{max} in MSW leachate. The double-sided immersion data and their fitting curves are from Abdelaal and Samea (2023) and Samea and Abdelaal (2023b).

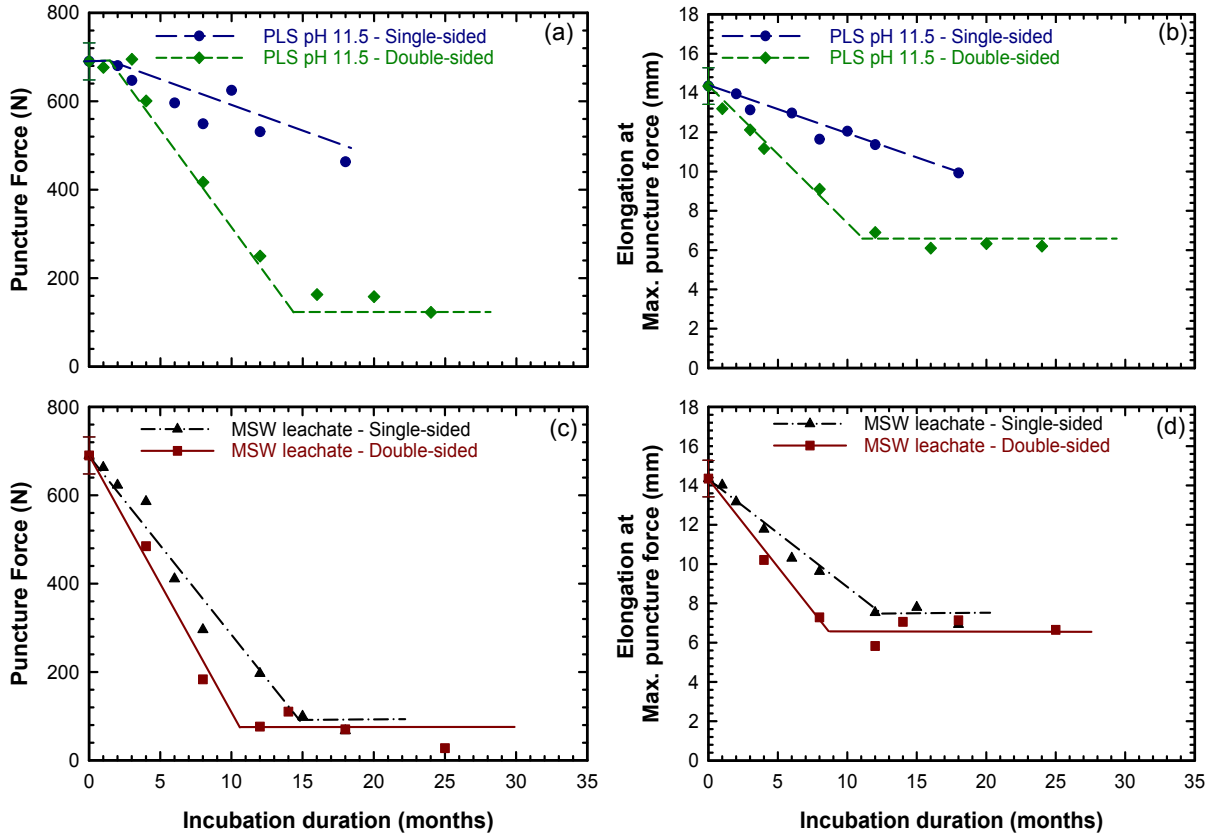

Figure 6. Variation of the puncture properties with incubation time at 70°C for double and single-sided immersion in PLS pH 11.5 and MSW leachate (a) peak puncture force in PLS pH 11.5; (b) elongation at peak puncture force in PLS pH 11.5; (c) peak puncture force MSW leachate; (d) elongation at peak puncture force in MSW leachate. The double-sided immersion data and their fitting curves are from Abdelaal and Samea (2023) and Samea and Abdelaal (2023b).

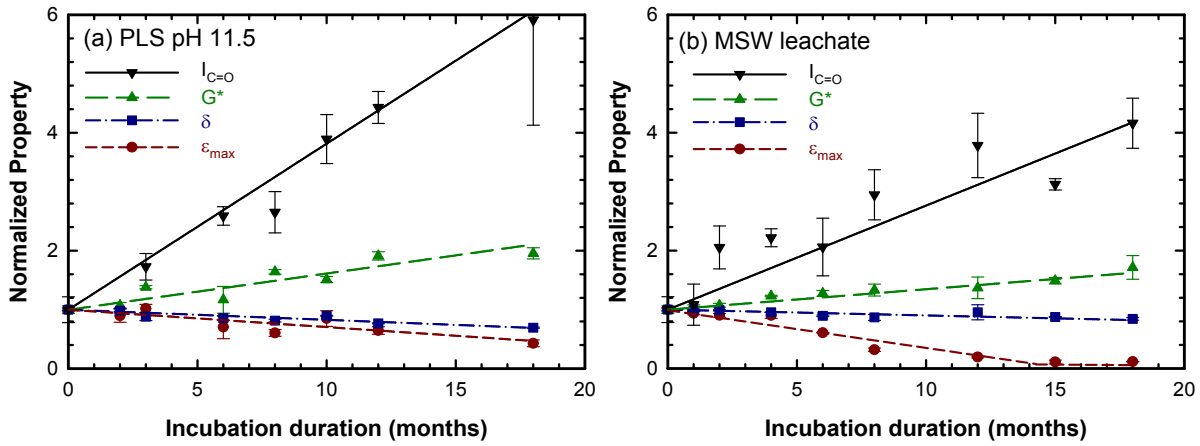

Figure 7. Variation of the different normalized properties (aged values/initial values) of the BGM with incubation time obtained from the single-sided immersion at 70°C in (a) PLS pH 11.5; (b) MSW leachate.

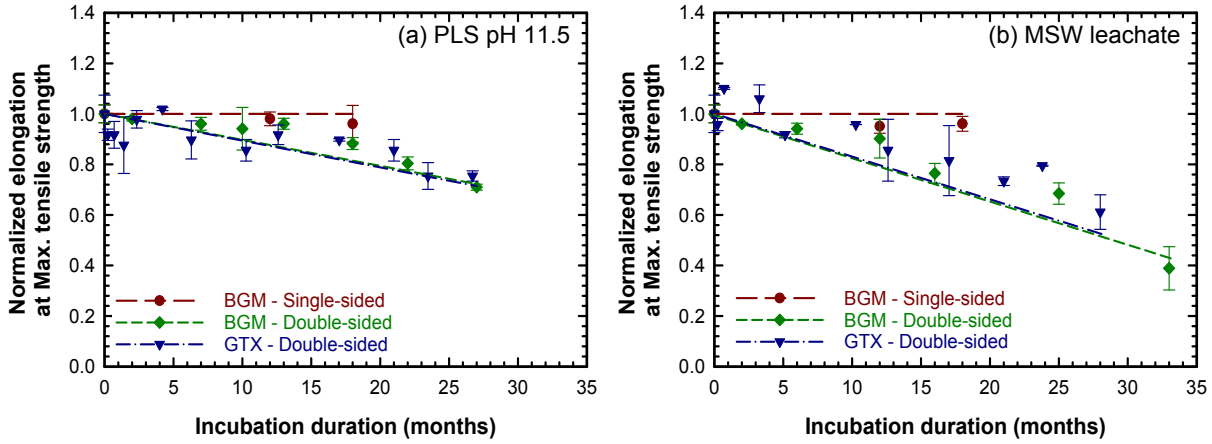

Figure 8. Variation in the normalized (aged values/initial values) elongation at maximum tensile strength (ε_{max}) with incubation time of the double-sided immersed BGM (with sealed edges), single-sided immersed BGM, and the NW-GTX samples at 55°C in (a) PLS pH 11.5; (b) MSW leachate. The double-side immersion data and their fitting curves are from Abdelaal and Samea (2023) and Samea and Abdelaal (2023b).

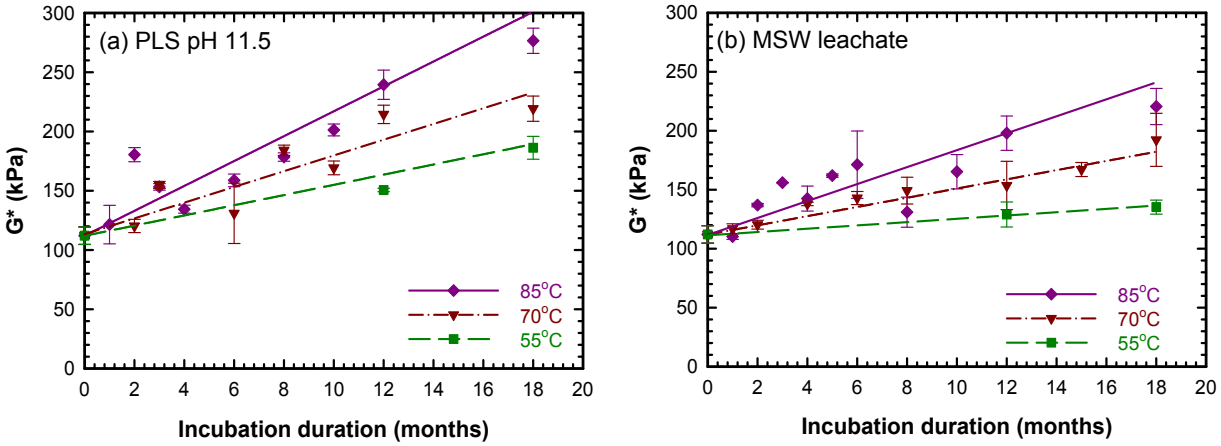

Figure 9. Variation of the complex shear modulus (*G) with the incubation time of the BGM at different temperatures in (a) PLS pH 11.5; (b) MSW leachate.**

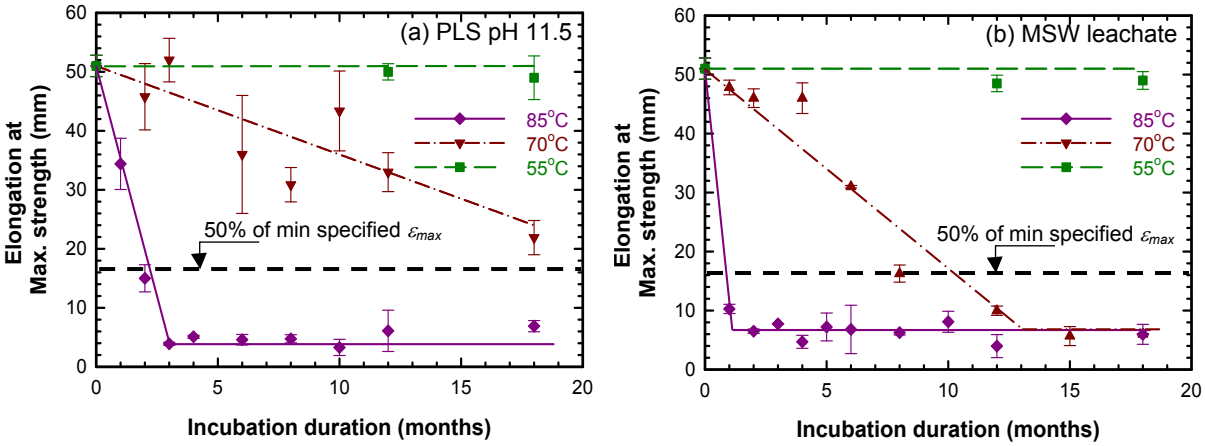

Figure 10. Variation of the elongation at maximum tensile strength (ε_{max}) with the incubation time of the BGM at different temperatures in (a) PLS pH 11.5; (b) MSW leachate.

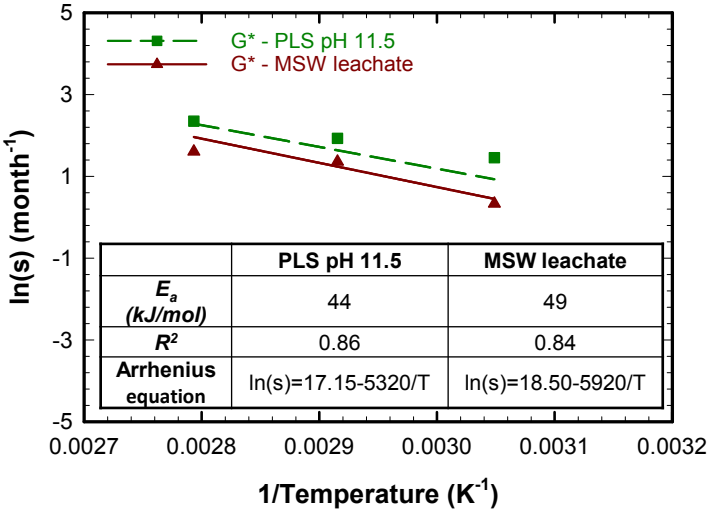

	PLS pH 11.5	MSW leachate
E_a (kJ/mol)	44	49
R^2	0.86	0.84
Arrhenius equation	ln(s)=17.15-5320/T	ln(s)=18.50-5920/T

Figure 11. Arrhenius plots of the complex shear modulus (*G) for the single-sided BGM samples immersed in PLS pH 11.5 and MSW leachate.**